Waste and Biomass Valorization
https://doi.org/10.1007/s12649-026-03686-w

ORIGINAL PAPER

Pilot-Scale Valorization of Food Waste using *Eucalyptus grandis*-Derived Biochar: Functional Roles in pH Modulation, Volatile Fatty Acid Dynamics, Microbial Network Transitions, and Preliminary Technoeconomic Assessment

Patrick T. Sekoai[1,2] · S'fiso Thuthukani Gumbi[3] · Olufemi Samson Egbewale[3] · Siphesihle Mbatha[4] · Refiloe Nyathela[1] · Nomathemba Makhapela[1] · Anish Ghimire[5] · Jonas Johakimu[2] · Viren Chunilall[2,6]

Received: 24 October 2025 / Accepted: 25 May 2026

Abstract
Biochar is increasingly recognized in biorefineries for its unique physicochemical properties that enhance microbial performance and process stability. However, limited research has examined its biocatalytic functions in food waste valorization, particularly in the Global South regions. This study investigates the functional roles of *Eucalyptus grandis*-derived biochar in a pilot-scale anaerobic system, emphasizing pH modulation, volatile fatty acids (VFAs) dynamics, microbial network transitions, and technoeconomic studies. Comprehensive biochar characterization using FTIR, BET, SEM, TGA, XRD, and CHNS analyses revealed favorable surface functionality, porosity, and nutrient content conducive to microbial colonization. Biochar addition maintained a stable pH range of 7.03–5.0, contrasting with the sharper decline observed in the control (7.03–4.30). Acetic acid was the dominant VFA, with a markedly higher relative proportion in the biochar-amended reactor (53.23%) than in the control (15.23%). Nutrient recovery in the resulting biofertilizer was also enhanced, attaining 92.12 ± 0.13, 682.08 ± 0.21, and 4238.06 ± 0.05 mg/L for nitrogen, phosphorus, and potassium (NPK), respectively. Enhanced VFA depletion indicated stimulated syntrophic activity, corroborated by microbial community analysis, which showed enrichment of *Pseudomonadota* and *Campylobacterota*, taxa pivotal to syntrophic metabolism and carbon flux regulation. Preliminary techno-economic studies also confirmed the cost-effectiveness of biochar in food waste biorefineries. These findings demonstrate that *Eucalyptus grandis* biochar functions as a sustainable, low-cost bioadditive that enhances biocatalytic efficiency and nutrient recovery in food waste valorization. This work establishes a scalable biorefinery model for a biochar-mediated bioprocess that advances circular bioeconomy principles and promotes environmental and socioeconomic resilience in developing regions.

Keywords Biochar · Food waste · Anaerobic co-digestion · Circular bioeconomy

✉ Patrick T. Sekoai
patricksekoai@gmail.com

[1] Department of Microbiology, Faculty of Natural and Agricultural Sciences, North-West University, Private Bag X2046, Mafikeng 2735, South Africa

[2] Biorefinery Industry Development Facility, Council for Scientific and Industrial Research, Durban 4041, South Africa

[3] Discipline of Microbiology, School of Life Sciences, University of KwaZulu- Natal, Westville Campus, Private Bag X54001, Durban 4000, South Africa

[4] School of Chemical and Minerals Engineering, Faculty of Engineering, North- West University, Private Bag X6001, Potchefstroom 2531, South Africa

[5] Environmental Engineering and Management, Asian Institute of Technology, Pathum Thani 12120, Thailand

[6] Discipline of Chemical Engineering, University of KwaZulu-Natal, Durban 4041, South Africa

Published online: 17 June 2026

Introduction

The challenges posed by the linear economy, including climate change, environmental pollution, water scarcity, food insecurity, and natural resource depletion, have thrust sustainable technologies to the forefront of global discourse. The circular bioeconomy has been identified as an innovative strategy for achieving this paradigm shift [1, 2].

The global community is also embracing this concept as fossil-intensive economies, including the European Union, have included it in their economic model as corroborated by the "Fit for 55" EU Plan, the EU Circular Economy Action Plan, and the EU Zero Pollution Action Plan, among others [3–5]. In the same vein, South Africa is following a similar technological roadmap as the world's 15th biggest fossil-based economy by advancing its circular bioeconomy innovations as shown by recent legislations such as the National Development Plan 2030, the Decadal Plan, the Bio-economy Strategy, the Waste Economy Master Plan, Forestry Bioeconomy Innovation Cluster, Industrial Biocatalysis Hub, and the White Paper on Science, Technology and Innovation [6].

Food waste has been the subject of major valorization research in recent years due to its desirable properties, including its carbohydrate-rich content, ubiquity, high biodegradability, renewability, and susceptibility to biochemical and chemical pretreatments [7]. This substrate fits well within the bioeconomy model as 1.3 billion tons are produced globally annually, implying that it is suitable for large-scale biorefineries [8]. South Africa is also experiencing a drastic increase in food waste production (10.3 million tons per annum) due to rapid population growth, food and beverage industry expansion, high agricultural outputs, and improved living standards [9]. Given the stringent environmental policies adopted by nations on the disposal of organic waste, adopting the food waste biorefinery concept will not only prevent environmental pollution but will also foster the creation of new biobased value chains from this copious waste stream.

Anaerobic co-digestion is regarded as the cornerstone for food waste biorefinery frameworks, providing affordable biobased value chains [10, 11]. It is a biochemical process that uses coordinated microbial communities spanning several taxonomic phyla to produce biobased products using different biodegradable wastes [12]. This technology coincides with the burgeoning global bioeconomy trends due to its (i) ability to valorize the overabundant biowaste streams, including industrial and municipal side streams (ii) contributions to the "waste-to-value" innovations (iii) contributions to social upliftment and economic development in marginalized communities (iv) ability to use mesophilic conditions as opposed to energy-intensive chemical processes (v) ability to co-produce biobased products using closed-loop biorefineries, and (vi) attainment of large-scale anaerobic systems which implies it is viable for industrial implementation [13].

Despite the technological strides that have been made in this scientific domain, anaerobic digestion processes still suffer from major scientific shortfalls, such as process instabilities resulting in low outputs and economic losses for industries. As a response to this barrier, scientists are proposing biochar as a suitable bio-additive. Biochar has garnered widespread attention in recent years due to its outstanding properties, such as high surface-area-to-volume ratio, high cation exchange capacity, and high adsorption abilities [14]. When applied as a stimulatory bio-additive in microbial-based biorefineries, it shortens the lag phase of the inocula, improves the hydrolysis of feedstocks, aids in maintaining favorable pH conditions, allows the fermenting microbes to resist toxic inhibitors, provides a balanced C/N ratio, promotes direct interspecies electron transfer (DIET), and promotes synergistic mechanisms among biofilm-forming communities [15].

This carbonaceous material remains an underutilized bioresource in developing nations like South Africa. Research shows that this biomass could immensely benefit South Africa, as vast biorefinery portfolios could be leveraged due to the country's forestry sector, which produces ~ 2.3 million m^3 of biowaste per annum [6]. Furthermore, the continuous production of forestry waste poses a serious threat to the environment as the industry only processes 40% of its initial biomass, implying that 60% of biomass remains unutilized and is often discarded in landfill sites, leading to various environmental hazards [16]. The *Eucalyptus* plant is an important source of hardwood timber in South Africa due to its acclimatization to the local climatic conditions, rapid growth, exquisite branch and stem properties, resistance to parasites and plant diseases, ease of cultivation, and ability to produce a wide spectrum of timber products [17]. Presently, more than 500,000 hectares of forest landscapes in South Africa are covered by *Eucalyptus* plantations [18]. Therefore, this forestry-based material is viewed as a crucial feedstock that will advance the production of valuable biobased resources such as biochar in South Africa.

We acknowledge that there has been an expanding scholarly body of knowledge regarding the use of biochar in this scientific domain. However, a significant focus is on improving biogas production outputs [19–24], and little attention is put on acquiring an in-depth understanding of its impact on liquid-phase parameters such as VFA concentration, biodigestate composition, and microbial population dynamics. Techno-economic forecasts also show that biogas alone yields low profits, necessitating the need to include

integrated biorefinery routes to maximize the recovery of other biocommodities [11].

Lou et al. [25] discovered that biochar accelerates the microbial conversion of substrates due to the enrichment of synergistic consortia, resulting in high VFAs [25]. Other authors reported that it enhances the acidogenic-solventogenic transition phase [26]. Therefore, these scientific variations underscore the need for further research to provide plausible explanations for these phenomena while reconciling these reports based on the studied biostimulatory effects of biochar on VFA and NPK outcomes. From a social standpoint, acquiring in-depth knowledge about the bioaugmentation role of biochar on these variables is critical as fermented effluents are renowned in the local agricultural communities as valuable fertilizers for improved soil quality and crop productivity. For further downstream processing, these VFAs can be purified and used as valuable precursors in other biorefinery routes such as chemical production, wastewater treatment, and biopolymer production [1], but this is outside the scope of this research.

In this pilot-scale study, we investigate the influence of wood-derived biochar on the anaerobic co-digestion of food waste, focusing on its role in stabilizing pH, enhancing volatile fatty acid (VFA) accumulation, improving biofertilizer nutrient composition, and modulating microbial community dynamics. This work aims to advance our understanding of biochar-mediated biorefineries within the context of circular bioeconomy and sustainable biorefinery applications. Specifically, the key objectives of the study are to: (i) produce biochar from locally sourced woodchips, (ii) characterize its key physicochemical properties, and (iii) employ it as a bio-enrichment additive in biocatalytic trials to evaluate its mechanistic effects on VFA production, pH regulation, nutrient recovery, and microbial ecological shifts during the closed-loop pilot-scale food waste valorization process.

Materials and methods

Raw Materials and Biochar Production

The South African *Eucalyptus grandis* woodchips were provided by Sappi Sawmill, Umkomaas, KwaZulu-Natal, South Africa. Prior to the pyrolysis step, the acquired woodchips, which had an average size of 3–6 mm, were air-dried to remove moisture. Subsequently, the biochar was produced using the bench-scale pyrolysis unit (Thermopower Furnace, Johannesburg, South Africa) at a pyrolysis temperature of 600 °C, as described in the study of Zhang et al. [27]. Figure 1 illustrates the adopted biochar-producing unit process operation for this conceptualized research study.

Biochar Characterization

Elemental Analysis

The elemental analysis was conducted to determine the composition of carbon (C), hydrogen (H), nitrogen (N), and sulfur (S) in biochar. This was facilitated using the Perkin Elmer 2400 Series II CHNS Analyzer (Perkin Elmer Inc., Waltham, USA) [28]. The fraction of oxygen was calculated by subtracting the content of C, H, N, and S from 100% [29].

Scanning Electron Microscopy Analysis

The surface morphology of the produced biochar was analyzed using a desktop scanning electron microscope (SEM) (Phenom Pharos, Thermo Fisher Scientific, Waltham, USA) at a voltage of 10 kV [30]. Before the SEM analysis, it was placed on a metal stub with the aid of carbon tape and subsequently covered with thin gold coating material using the Q150RES sputter coater (Quorum Technologies, UK), as shown in the literature [30].

Fourier-Transform Infrared Analysis

To determine the functional groups present in the biochar, it was measured using a 100 FTIR Spectrophotometer (PerkinElmer, Waltham, USA). The scanning conditions were in the spectral range of 4000–500 cm^{-1} and with a resolution of 4 cm^{-1}.

Thermal Gravimetric Analysis

The thermal gravimetric analysis (TGA) was conducted using the STA 6000 Simultaneous Thermal Analyzer (PerkinElmer, Waltham, USA) under an ambient atmosphere of dry nitrogen set at a flowrate of 10 °C/min and a temperature range of 35–800 °C [30].

X-ray Diffractometer (XRD) Analysis

The crystallographic properties of the wood-derived biochar were analyzed using an X-ray diffractometer (PANalytical X'Pert Pro, Netherlands) operated at a Cu-Kα radiation (λ = 1.5406 Å) with a filament intensity of 40 mA and a voltage of 45 kV.

Brunauer-Emmett-Teller (BET) Surface Analysis

The BET surface area, pore size, and volume were measured using nitrogen at 77 K using the BET instrument (Micromeritics TriStar II 3020, GA, USA). Prior to the

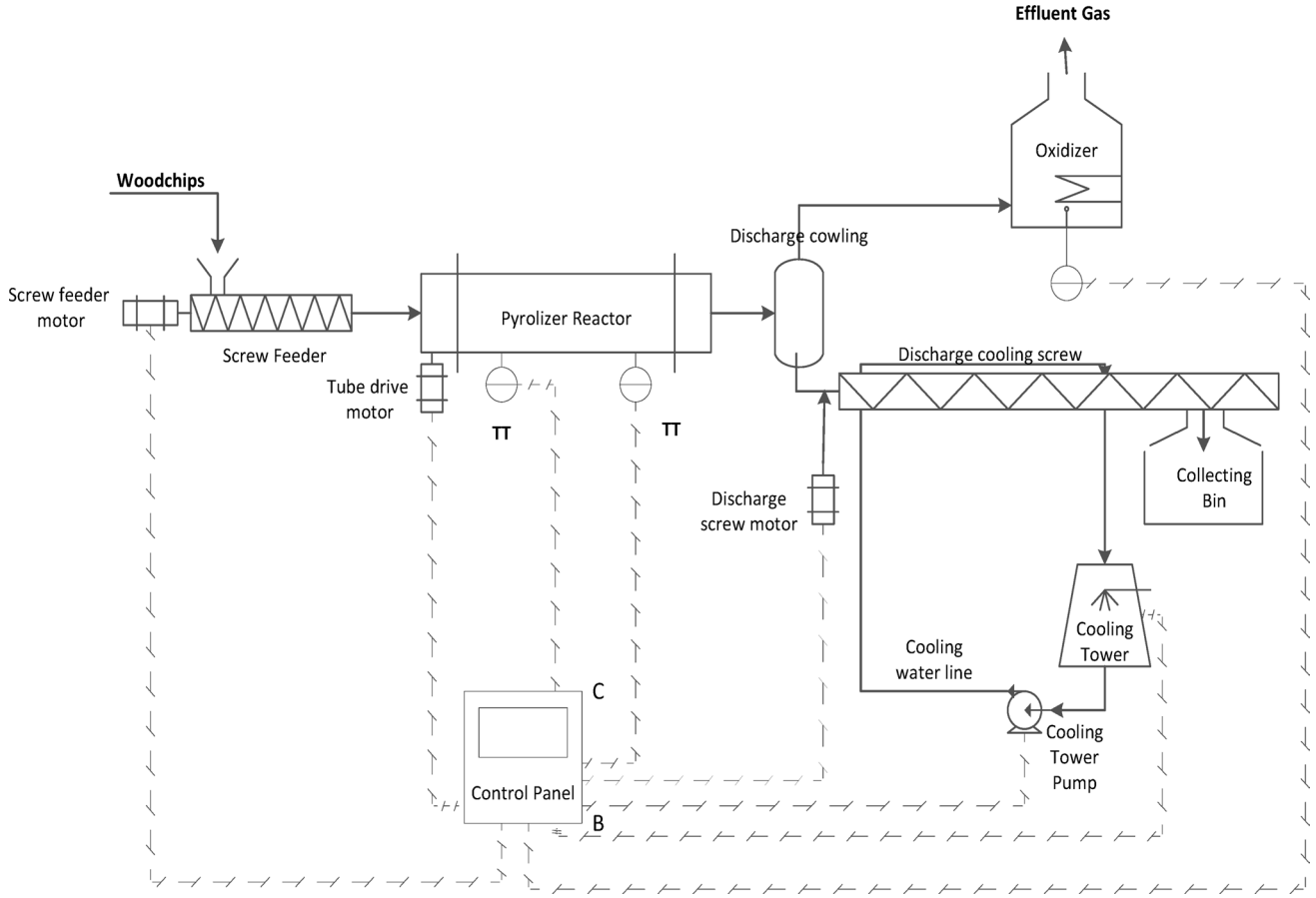

Fig. 1 Schematic depicting the bench-scale pyrolysis unit set-up

analysis, the biochar was degassed at 90 °C for 1 h, followed by heating at 200 °C for 5 h.

Collection of Feedstocks and Biocatalytic Trials

Feedstock Acquisition and Pretreatment

The food waste was collected from a local food vendors' market, which is situated 5 km from our research facility. It consisted solely of fruit and vegetable waste, and these feedstocks have been shown to promote the growth of diverse anaerobic cultures due to their rich carbohydrate content [31]. It was brought into our laboratory using sealed plastic containers. After this step, it was reduced to small particles (3 mm) using a kitchen blender before the anaerobic digestion trials, as reported in the literature [32]. Additionally, the fresh cow dung was collected from a free-range grazing cow farm in uMsunduzi, KwaZulu-Natal, in South Africa. It was selected as it harbors microorganisms spanning versatile taxonomic divisions of fermentative assemblages such as hydrolytic bacteria, acidogenic species, acetogenic species, and methanogenic species [33]. The nutritional properties of food waste and cow dung were chemically screened to confirm their suitability for anaerobic food waste digestion.

Pilot-Scale Biocatalytic Experiments

The anaerobic fermentation experiments were conducted via the co-digestion approach involving cow dung and food waste as shown in our previous study [34]. Herein, a co-digestion mass ratio of 50:50 was chosen for cow dung and food waste as this was proven to yield a better performance [34]. The food waste upcycling experiments were conducted using the commissioned 1000 L anaerobic pilot-scale fermenter. The anaerobic digestion trials included two treatments; the control experiment consisted of only cow dung and food waste, while the biochar-mediated experiments consisted of cow dung and food waste as co-digested feedstocks coupled with biochar as a 0.5% w/v bio-additive [14]. The fermenter was fed with equal mass proportions of cow dung (50 kg) and food waste (50 kg) and filled with 700 L of water, except for the control experiment in which the biochar was not added. The anaerobic co-digestion process was conducted for 30 days (in replicates) in ambient atmospheric (20–35 °C) conditions without any external pH

regulation. The pilot-scale biodigester was stirred manually once daily using a hand-operated stirrer to facilitate homogeneity. Five milliliters of effluent were sampled daily from the fermenter for biochemical and microbial analyses.

Microbial Community Profiling

Sludge samples from anaerobic digesters were homogenized on a Tissue Lyser II (Qiagen) with 5 mm stainless steel beads for 3 min at 25 Hz and 4 °C to ensure consistent disruption without thermal damage. The homogenate was diluted 1:1 with sterile PBS (pH 7.4) and centrifuged at 500 × g for 10 min at 4 °C to remove macro-debris. Microbial cells were pelleted by centrifugation at 10,000 × g for 15 min at 4 °C, washed twice with PBS to eliminate PCR inhibitors, and immediately subjected to DNA extraction.

Genomic DNA was isolated using the DNeasy PowerSoil Pro Kit (Qiagen) with an extended 20 min lysis step and an additional phenol–chloroform cleanup to remove humic acids and biochar-associated contaminants. Extracted DNA quality was confirmed by Qubit fluorometry and NanoDrop spectrophotometry, targeting A260/A280 ratios > 1.8 and A260/A230 ratios > 2.0. Each extraction batch included six negative controls and a ZymoBIOMICS microbial standard as a positive control. Inhibition was evaluated by spiking serially diluted samples with an internal amplification control.

The V3–V4 regions of the 16 S rRNA gene were amplified with primers 341 F (5′-CCTACGGGNGGCWGCAG-3′) and 805R (5′-GACTACHVGGGTATCTAATCC-3′), each flanked by Illumina adapter sequences. PCR reactions (25 µL) used KAPA HiFi HotStart DNA polymerase under the following cycling conditions: 95 °C for 3 min; 25 cycles of 95 °C for 30 s, 55 °C for 30 s, 72 °C for 30 s; final extension at 72 °C for 5 min. Triplicate amplifications per sample were pooled, purified with AMPure XP beads (0.8×), and quantified by Qubit. Indexed libraries were constructed using the Nextera XT Index Kit and sequenced on an Illumina MiSeq (2 × 300 bp), targeting 50,000 paired-end reads per sample. Full-length 16 S rRNA gene amplicons were sequenced on the PacBio Revio Platform (Pacific Biosciences, Menlo Park, CA, USA), which provides long, high-fidelity reads that enhance taxonomic resolution compared with short-read technologies [80]. Long-read sequencing data were processed using the SMRTLink software suite (v25.1.0.257715, Pacific Biosciences). Subreads were converted into highly accurate consensus sequences (QV > 40) using the Circular Consensus Sequencing (CCS) algorithm [11]. Amplicon sequence processing for both short- and long-read datasets was performed with DADA2, which denoised reads, removed low-quality and chimeric sequences, and resolved amplicon sequence variants (ASVs) at single-nucleotide resolution [7]. Quality-filtered ASVs were classified in QIIME 2 (v2021.11) against reference databases optimized for full-length 16 S rRNA sequences, enabling taxonomic resolution from kingdom to species level. The raw Illumina MiSeq and PacBio Revio 16 S rRNA sequencing reads have been deposited in the NCBI Sequence Read Archive under BioSample accessions SAMN56514214 and SAMN56514215, respectively.

Raw Illumina reads were further processed in QIIME 2 (v2023.5) following established protocols. Quality filtering retained reads with a minimum Phred score of 20 and a maximum expected errors of 2.0. Taxonomic assignments used the SILVA 138 classifier at 99% confidence [7]. Sequences were aligned via MAFFT [10], and a phylogenetic tree was inferred using FastTree [10]. Alpha diversity metrics (Shannon, Simpson, Chao1) were calculated in R using the vegan package [12]. Normality was assessed by Shapiro–Wilk tests. P-values were adjusted using the Benjamini–Hochberg false discovery rate method. Beta diversity was quantified using weighted and unweighted UniFrac distances. Community structure differences were tested via PERMANOVA (adonis2, 999 permutations) with Bonferroni correction. DESeq2 performed differential abundance analysis on ASVs present in > 25% of samples with mean relative abundance > 0.1%. Counts were normalized by the geometric mean, and taxa with $|\log_2$ fold-change$|>1.5$ and adjusted $p < 0.05$ were considered significant. Negative extraction and PCR controls were sequenced to identify contaminant ASVs. Any ASV detected in controls was removed from sample datasets unless its abundance in samples exceeded control levels by at least tenfold. ZymoBIOMICS mock communities were processed in parallel to benchmark sequencing accuracy; observed versus expected compositions were compared using Bray–Curtis dissimilarity. Reproducibility was ensured by standardized protocols and independent duplication of a subset of 12 samples by different operators, yielding intraclass correlation coefficients > 0.85 across diversity metrics.

The Techno-Economic Analysis

The techno-economic analysis is considered in this study, which includes both the capital and operational expenditure cost items to assess the profitability of the biochar-mediated process. Operational expenditure cost includes variable costs, i.e., the labour cost, electricity, etc. The capital cost will include the fixed costs. The total cost (TC), a sum of all costs, is calculated using Eq. 1. The total income (Revenue) is calculated considering the selling price (SP) of biofertilizer and biogas using Eq. 2. Thereafter, the net/total profit (NP) is calculated using Eq. 3.

$$\mathrm{TC} = \sum (\text{Raw Material Cost, Operating Cost, Utilities Cost}) \quad (1)$$

$$\text{Revenue} = \sum SP_i \times F_i \times OPH \quad (2)$$

$$\mathrm{P} = \text{Revenue} - -\mathrm{TC} \quad (3)$$

Where F_i is the total component i (biofertilizer, biogas) production flowrate and OPH is the total operating hours.

Analytical Methods

The VFAs comprising acetate, butyrate, propionate, isobutyrate, and hexanoate were measured using the Agilent 6890 Gas Chromatograph (Agilent Technologies, CA, USA) fitted with the ZB FFAP column (60 m x 0.32 mm). Helium was used as a carrier gas at a flow rate of 2.9 mL/min as reported in our previous study [34]. The concentrations of phosphorus (P) and potassium (K) present in the effluents were determined using the method described by Khayum et al. [35], while the nitrogen (N) was calculated using the Perkin Elmer CHNS Analyzer as stated in Sect. 2.2.1. The pH was measured using the bench-top pH Meter (Metrohm, Woodmead, South Africa). The concentrations of carbohydrates in food waste and cow dung were analyzed using the Dionex ICS 5000 + HPIC System (Thermo Fisher Scientific, Massachusetts, USA). The fractions of the inorganic compounds, including the trace metals studied, were analyzed using the TAPPI Method [36]. The total organic content fraction was determined by subtracting the total inorganics from 100% as reported in the literature [36]. Meanwhile, the fat and protein content were calculated according to the literature [37]. The cellulolytic enzyme activity was measured using the procedure described by Fung et al. [11].

Results and Discussion

Biochar Production Yield

In this study, the biochar yield was determined to be 35.9%. This value coincides with findings from other researchers who have reported biochar yields ranging from 20% to 50% when employing different lignin-rich feedstocks [38–41]. This was also consistent with other scientific studies that observed that high pyrolysis temperatures significantly affect biochar yields, primarily due to the enhanced thermal decomposition of the feedstock materials. While there is no direct correlation established between biochar yield and its impact on anaerobic digestion, research conducted by Alghashm et al. [42] indicates that biochar produced at specific temperature ranges can enhance anaerobic fermentations. This observation was confirmed in several outcomes, including (i) a reduction in the lag phase, (ii) an increase in the production and conversion of volatile fatty acids (VFAs), (iii) improved chemical oxygen demand (COD) removal, and (iv) augmented biogas production [42]. These improvements are likely caused by high porosity and aromaticity originating from the elevated pyrolysis temperature.

Calorific Value of Biochar

The calorific value, also known as the heating value, is one of the pyrolytic outputs used to gauge the applicability of biochar in fuel applications [43]. Interestingly, the biochar obtained in this study had a heating value of 26,33 MJ/kg, which is higher than that of coal (23 MJ/kg). This implies that it can serve as a substitute for coal [44, 45]. These results are consistent with scientific literature, as it was reported that biochars produced from *Eucalyptus* biomass have heating values of 25–35 MJ/kg [46, 47]. Woody materials have a high content of carbonyl and hydroxyl groups, which contribute to the overall chemical properties of wood-based biochar, including their heating values [48].

Physicochemical Characterization of Biochar

To acquire in-depth insights into the biostimulatory role of wood-derived biochar in food waste valorization, it is crucial first to explore its physicochemical properties and elucidate how these affect the biocatalytic valorization of food waste. This was achieved by subjecting the biochar to several key characterization tests as articulated below.

SEM Analysis of Biochar

The biochar consisted of distinctive honeycomb-like pore structures as a result of the thermal depolymerization of the chemical compounds present in the raw biomass, as shown in Fig. 2. Higher carbonization temperatures (exceeding 400 °C) tend to enhance porosity and promote the formation of aromatic compounds within the biochar, which is caused by an increase in the carbon stability of the final product [49–51]. These findings correlate with literature. Sahoo et al. [38] and Yargicoglu et al. [52] observed similar SEM micrograph patterns in forestry-based biochars. In addition, biochars produced from forestry residues typically exhibit larger pore sizes due to their high chemical composition of lignin, hemicellulose, and cellulose [46, 53], as evidenced in this study. Elsewhere, it was reported that biochars produced at high temperatures are ideal as they result in more porous structures with large surface areas, which in turn enhance microbial aggregation, biofilm formations, water retention, pollution removal, and adsorption capabilities, making them attractive for a wide spectrum of microbial-based

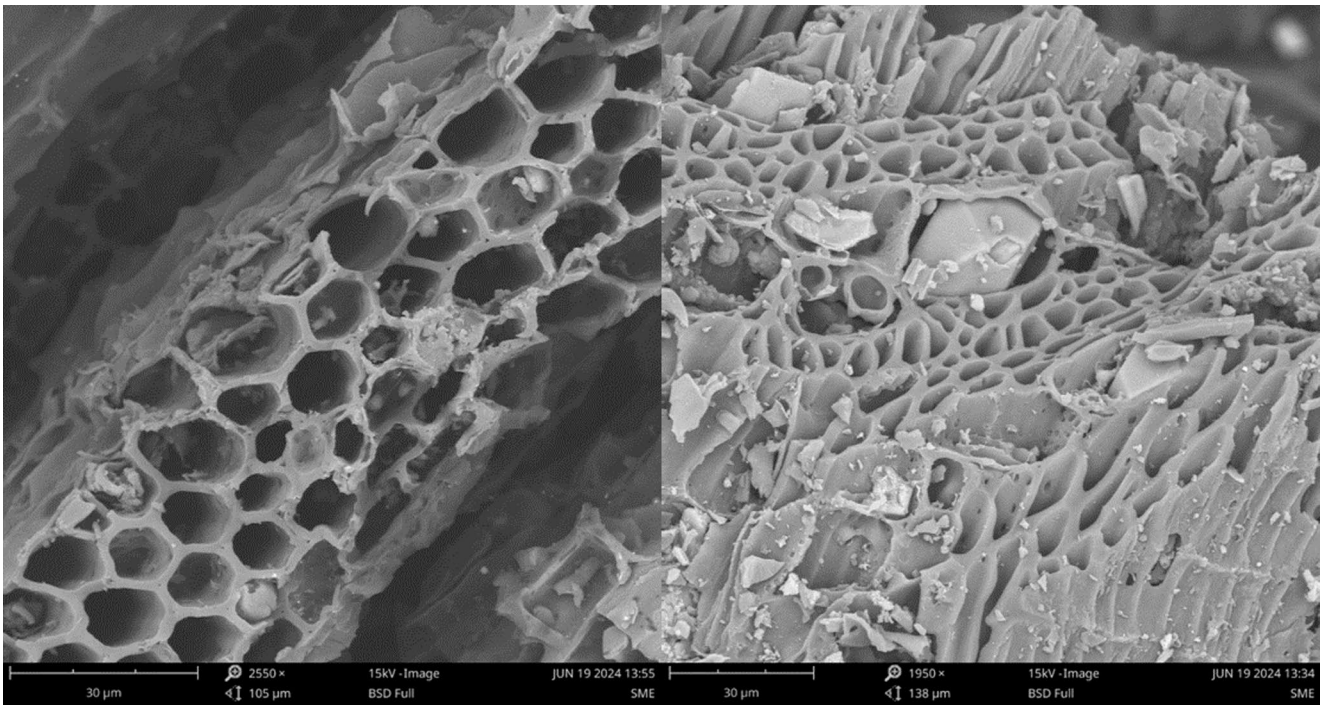

Fig. 2 The scanning electron micrographs of the biochar sample

Table 1 Elemental composition of biochar

Sample	C (%)	H (%)	*N* (%)	S (%)	O (%)	H/C	O/C
Biochar	69.42	2.18	0.23	0.72	27.45	0.03	0.40

biorefineries [54]. For this reason, the selection of the pyrolytic feedstock should not be overlooked as lignin-rich feedstocks contribute to the thermal stability of biochar due to the formation of stable C-C bonds with 5–5 linkages in comparison to hemicellulose- and cellulose-rich materials which produce less stable volatile compounds [55, 56].

Elemental Analysis of Biochar

Investigating the elemental composition in biochar is essential as these molecules affect the chemical stability of biochar [57]. The N and S atoms are considered minor elements due to their minor role in the stability of biochar; thus a major focus is put on carbon (C), hydrogen (H), and oxygen (O) elements as these affect the aromaticity and unsaturation of biochar based on their H/C and O/C ratios [41]. In this work, the biochar consisted primarily of C (69.42%) and a small fraction of H (2.18%), and these elements were used in determining an H/C ratio of 0.03 (Table 1). These results correspond with the literature as the process of pyrolysis promotes the dehydration and deoxygenation reactions, leading to the accumulation of stable C atoms in the biochar [58, 59]. Biochars with low H/C ratios, as also attested in this study, are indicative of high aromatic structures and high thermal stability [58, 60]. Meanwhile, the O/C ratio is used to measure the hydrophilicity of the biochar [61]. The low O/C ratio of 0.40 obtained in this work implies that the produced biochar is less hydrophilic. This observation is consistent with the literature as it has been reported in similar studies that increasing the pyrolysis temperature (300–700 °C) results in low O/C ratios due to a substantial loss in the oxygen-containing functional groups i.e., carbonyl, hydroxyl, and carboxyl groups [62].

FTIR Analysis

To delve deeper into its molecular constituents, the wood-derived biochar was subjected to further characterization tests in order to identify the main functional groups present in the studied biochar, as depicted by the FTIR wavelength spectrum in Fig. 3. This analytical test is critical for revealing the absorption pattern of the functional groups as a result of the thermal decomposition process [63]. The biochar exhibits typical spectra that correspond to lignocellulosic-rich biomass [50]. The peak at 3234 cm^{-1} is assigned to stretching vibrations of the O-H groups as these usually fall within the 3500–3000 cm^{-1} range in wood-derived biochars. The peaks at 1799 cm^{-1} and 1578 cm^{-1} are associated with the carbonyl C=O and aromatic C=C stretching vibrations, respectively. The peak at 1405 cm^{-1} represents

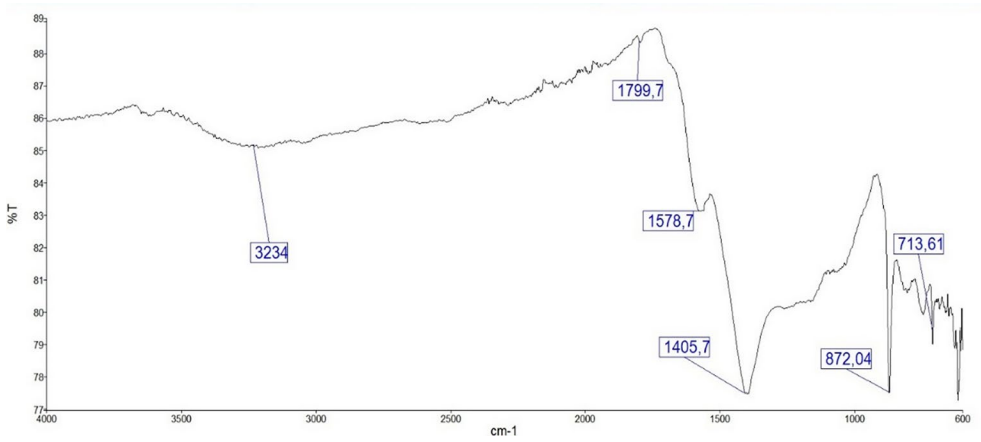

Fig. 3 FTIR spectra of the prepared wood-derived biochar

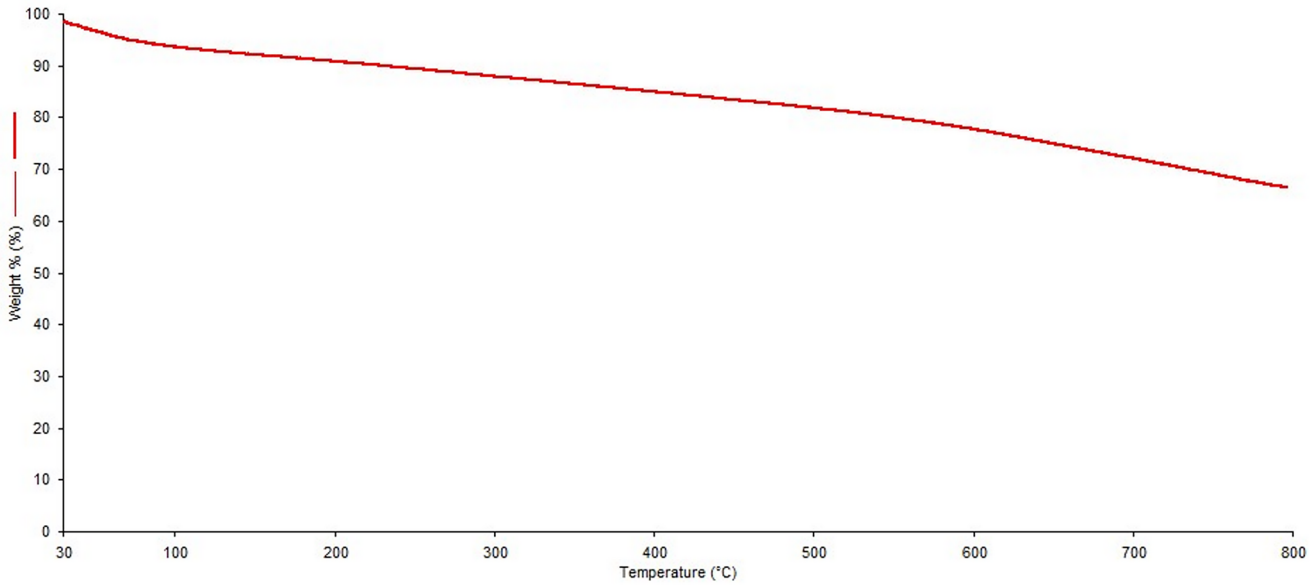

Fig. 4 TGA curve of the prepared wood-derived biochar

the aromatic ring structures, while the spectral peaks at 872 and 713 cm^{-1} represent the C-H bond in aromatic and heteroatomic compounds [38].

TGA Analysis

The TGA curve in Fig. 4 represents the material (weight) loss of the wood-derived biochar. The curve showed an acceptable weight loss of 32% induced by the pyrolysis temperature of 600 °C. It can therefore be deduced that the wood-derived biochar is thermally stable, as similar weight loss patterns were reported in the literature when using similar biomass and pyrolysis conditions [64]. Lignin-rich feedstocks constitute a rigid cross-linked structure compared to the low lignin-containing feedstocks, which produce unstable carbon and volatile compounds that are lost during the pyrolysis process [64].

XRD Analysis

As shown in Fig. 5, distinct peaks were observed at 2θ values of 23.52 and 29.38°, and these typically depict the crystal plane for cellulose and calcite, respectively [64]. The observed XRD patterns are similar to those of Sahoo et al. [38], who observed the crystallographic orientation of cellulose at 22.58° for wood-derived biochars and also reported that increasing the fractionation temperature led to the loss of the crystalline materials of cellulose due to the formation of miscellaneous inorganic compounds [38]. Minor XRD peaks were detected at 35.92–48.31°, which also represents the different chemical compounds in biochar, as corroborated in the study of Liu et al. [65].

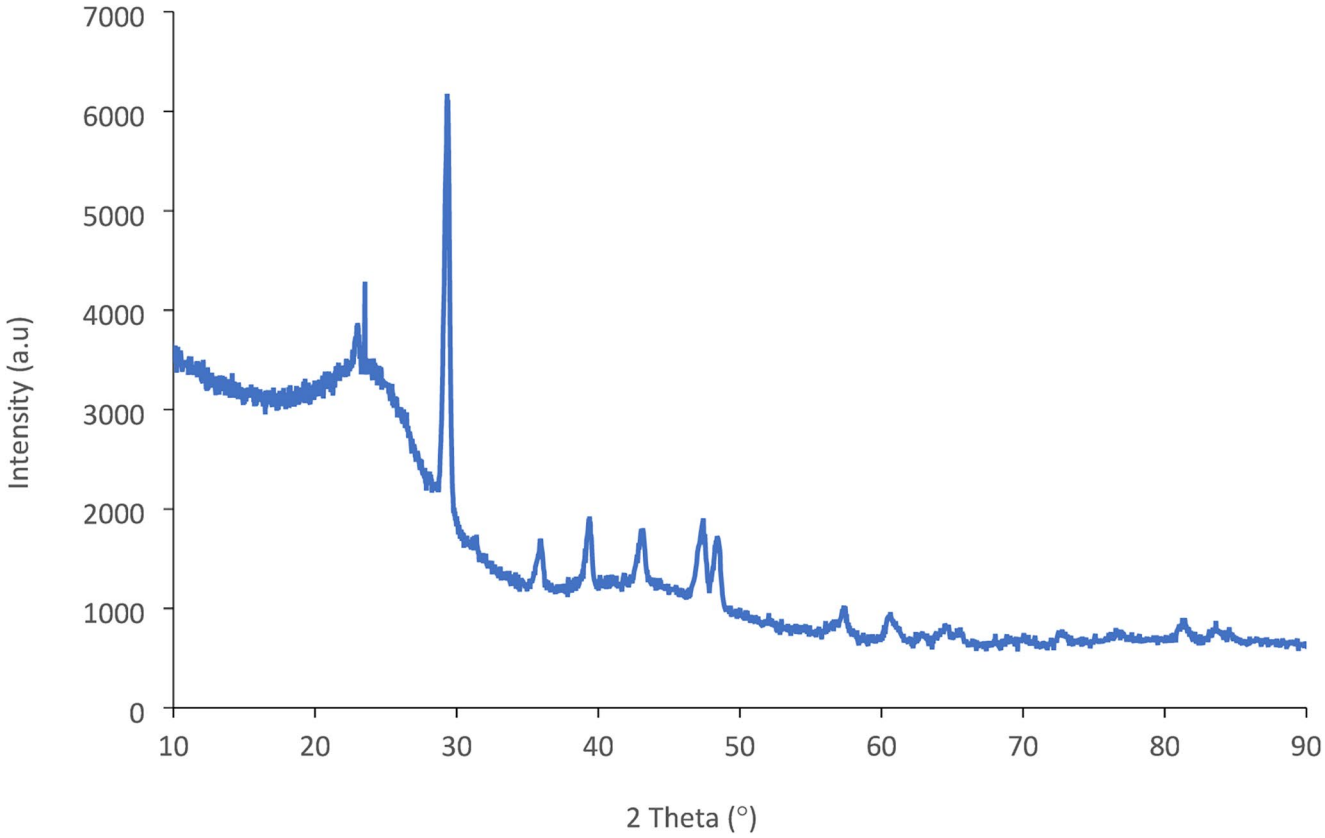

Fig. 5 XRD spectra of the prepared wood-derived biochar

Table 2 BET results of the wood-derived biochar

	BET surface area (m^2/g)	Total pore volume (cm^3/g)	Mean pore diameter (nm)
Biochar	140.29	0.10	2.0

BET Analysis

The wood-derived biochar possessed a specific surface area of 140.29 m^2/g, a total pore volume of 0.10 cm^3/g, and an average pore diameter of 2.0 nm, as shown in Table 2. This elevated surface area is consistent with previous research that documented BET surface areas ranging from 186.08 to 307.10 m^2/g when pyrolysis temperatures were maintained between 500 °C and 600 °C [38]. The pore volume and mean pore diameter are also in agreement with literature findings [38], where similar values were observed at elevated pyrolysis temperatures, attributed to the thermal degradation and subsequent release of vaporous organic compounds from the lignin-rich *Eucalyptus grandis* feedstock.

Chemical Characterization of Biochar via the Py-GC/MS

An additional analytical step was performed to assess other vital chemical constituents found in the wood-derived biochar using pyrolysis-gas chromatography/mass spectrometry (Py-GC/MS), as shown in Table 3. The biochar exhibited a high ketone content of 80.6%, which may be closely linked to the adopted pyrolysis setpoint conditions, which thermally disrupted the recalcitrant forestry-based structure. Biochars rich in aldehydes, hydroxyls, and ketones have been shown to possess high surface binding capabilities, particularly on polar contaminants [66]. As a consequence, it has been proposed that biochars exhibiting these chemical components may be applicable in bioremediation studies due to their high chelating strength [66]. This may create an opportunity for new scientific frontiers as this domain is still in its nascent stages.

Biocatalytic Valorization of Food Waste

Characteristics of Feedstocks used in Biocatalytic Trials

The nutritional compositions of the carbon and inoculum source utilized in the biocatalytic experiments are presented

Table 3 Chemical compounds present in biochar

Ketones	Retention Time	Area%	Name
	2.107	80.25	Stigmastane-3,6-dione, (5.alpha.)-
	2.785	0.35	2-PENTANONE
Total		80.6	
Ester	Retention Time	Area%	Name
	4.839	0.8	1,2,4-Benzenetricarboxylic acid, 1,2-dimethyl ester
	12.819	0.13	Carbonic acid, nonyl vinyl ester
	23.198	0.38	Sulfurous acid, hexyl octyl ester
Total		1.31	
Aldehyde	Retention Time	Area%	Name
	8.602	0.48	Benzaldehyde
	33.998	1.03	Butyraldehyde, semicarbazone
Total		1.51	
Alkene	Retention Time	Area%	Name
	9.996	0.25	Decane, 5-methyl-
	10.255	0.37	Decane, 4-methyl-
	11.305	0.58	Tetradecane
	12.648	0.61	Tetradecane
	14.475	0.18	DECANE, 2,9-DIMETHYL-
	15.527	0.68	DODECANE
	15.926	0.25	Undecane, 2,6-dimethyl-
	16.159	0.28	Tetradecane
	16.771	0.29	1-Iodo-2-methylundecane
	17.336	0.46	Undecane, 4-ethyl-
	17.778	0.76	Heptadecane
	19.036	0.42	Heptadecane
	20.986	0.58	Tetradecane
	21.544	0.29	Hexadecane
	22.328	0.36	Hexadecane
	22.554	0.16	Hexadecane
	23.267	0.18	Decane, 5-ethyl-5-methyl-
	23.394	0.96	Hexadecane
	24.475	0.51	Octadecane
Total		8.17	
Siloxanes	Retention Time	Area%	Name
	9.455	0.82	trisiloxane, 1,1,1,5,5,5-hexamethyl-3-[(trimethylsilyl)oxy]-
	14.115	0.56	Cyclopentasiloxane, decamethyl-
	18.931	0.91	Cyclohexasiloxane, dodecamethyl-
	23.324	0.49	3-Isopropoxy-1,1,1,7,7,7-hexamethyl-3,5,5-tris(trimethylsiloxy)tetrasiloxane
	30.641	0.45	Cyclohexasiloxane, dodecamethyl-
Total		3.23	
Nitrile	Retention Time	Area%	Name
	5.821	0.40	4-(METHOXYMETHYL)-6-METHYL-2-PHENOXYNICOTINONITRILE
Total		0.40	
Aromatics	Retention Time	Area%	Name
	2.599	1.00	Benzene
	3.894	0.48	Benzene, methyl-
	6.063	0.52	Benzene, 1,2-dimethyl-
	6.625	1.27	Benzene, ethenyl-
	12.432	0.31	Benzene, 1-methyl-4-(1-methylethenyl)-
Total		3.58	
Alcohol	Retention Time	Area%	Name
	15.31	0.34	1-nonanol
Total		0.34	
Cycloalkenes	Retention Time	Area%	Compound Name
	10.527	0.46	Cyclohexene, 1-methyl-4-(1-methylethenyl)-, (S)-

Table 3 (continued)

Ketones	Retention Time	Area%	Name
	2.107	80.25	Stigmastane-3,6-dione, (5.alpha.)-
	10.527	0.40	Cyclohexene, 1-methyl-4-(1-methylethenyl)-, (S)-
Total		0.86	

Table 4 Nutritional composition of feedstocks

Parameter	Food waste	Cow dung
Moisture (%)	17.60	14.88
Ash (%)	9.88	21.30
Inorganics (%)	9.88	21.30
Organics (%)	90.12	78.70
Calcium (mg/kg)	2 891	12 044
Potassium (mg/kg)	24 482	5 628
Magnesium (mg/kg)	1 076	5 026
Sodium (mg/kg)	3 445	843.0
Aluminium (mg/kg)	7.40	62.03
Barium (mg/kg)	0.870	6.63
Copper (mg/kg)	0.10	1.00
Iron (mg/kg)	5.85	48.14
Manganese (mg/kg)	2.95	24.54
Zinc (mg/kg)	0.95	9.00
C/N ratio	25.79	19.00
Protein (%)	11.12	11.33
Fat (%)	1.08	4.21
Carbohydrate (%)	65.18	45.08

in Table 4. It can be shown from nutritional results that food waste and cow dung are excellent feedstocks for the pursued biorefinery process. Food waste has a high biodegradable matter content of 90.12%, while cow dung contains 78.70% (Table 4). This high organic composition is essential for fostering the cultivation of syntrophic microorganisms including hydrolytic species, acidogens, acetogens, and methanogens. These biocatalysts thrive in anoxic microenvironments, which in turn stimulate the production of VFAs, biofertilizers, and other valuable compounds [8].

Furthermore, these findings coincide with existing literature that reports desirable concentrations of organic matter when utilizing comparable feedstocks in microbial-based biorefineries [9]. The results are further substantiated by the significant carbohydrate composition observed, measuring 65.18% for food waste and 45.08% for cow dung, respectively. Recent communications have shown that substrates rich in carbohydrates promote the growth of anaerobic microbial consortia more effectively than those rich in lipids and fats due to their inherent building blocks, which mainly consist of C_5 and C_6 sugar monomers [7, 9]. The carbon-to-nitrogen (C/N) ratios for food waste and cow dung were recorded as 25.79% and 19.00%, respectively. In literature, a C/N ratio within the range of 20–30 is ideal for sustaining a favorable nutritional equilibrium and enhancing the activities of potent microbes during food waste valorization [10]. Additionally, these feedstocks contain essential trace elements, including calcium, copper, iron, manganese, and magnesium, which confer stimulatory effects on biochemical pathways [10].

pH Profile During Biocatalytic Valorization Trials

Figure 6 illustrates the pH profile for biochar-treated and control experiments. In the control experiments, the pH varied from 7.03 to 4.30. This low pH range is primarily attributed to the rapid accumulation of VFAs and alcohols due to the bioprocess's minimum buffering capacity. This causes a drastic shift in the ecological niche of fermentative consortia due to the predominance of anaerobic inhibitors [66].

A similar occurrence was reported by Logan et al. [67] in a non-buffered anaerobic digestion system where the pH was below 5.5. Upon adding the biochar, an optimal pH range of 7.06–5.50 was attained during the 15-day fermentation period (Fig. 6). This phenomenon can be linked to the functional groups identified in the FTIR spectra, notably the hydroxyl (-OH) and carboxyl (-COOH) groups at 3243 cm^{-1}, which contribute to the buffering capacity acting as either weak acids or bases, which can accept protons (H^+) from the medium when pH decrease or release H^+ ions when the pH rises, thus resisting drastic pH changes in acidity. This proton exchange mechanism neutralizes excess acids generated during the anaerobic digestion period, as shown in Fig. 6 [66, 67]. Similar beneficial pH-buffering effects of biochar functional groups have been reported in the literature, further corroborating these findings. For example, Poerschmann et al. [68] and Gao et al. [69] observed that biochar provides a near-neutral pH range due to improved buffering and resistance to metabolic inhibitors and stresses. It is also worth highlighting that the neutral pH range is critical during anaerobic fermentations as it provides a good balance between the acidogenic–methanogenic transition pathway, and this ensures that the byproducts of acidogenic metabolisms serve as vital precursors for archaeal populations, as revealed by Jiang et al. [70] and Yellezuome et al. [71]. Acidic pH tends to disrupt the cell membranes of microorganisms, cause microbial stress, and reduce enzymatic functions, which in turn leads to the suppression of the methane-forming communities during the final step of anaerobic digestion [71].

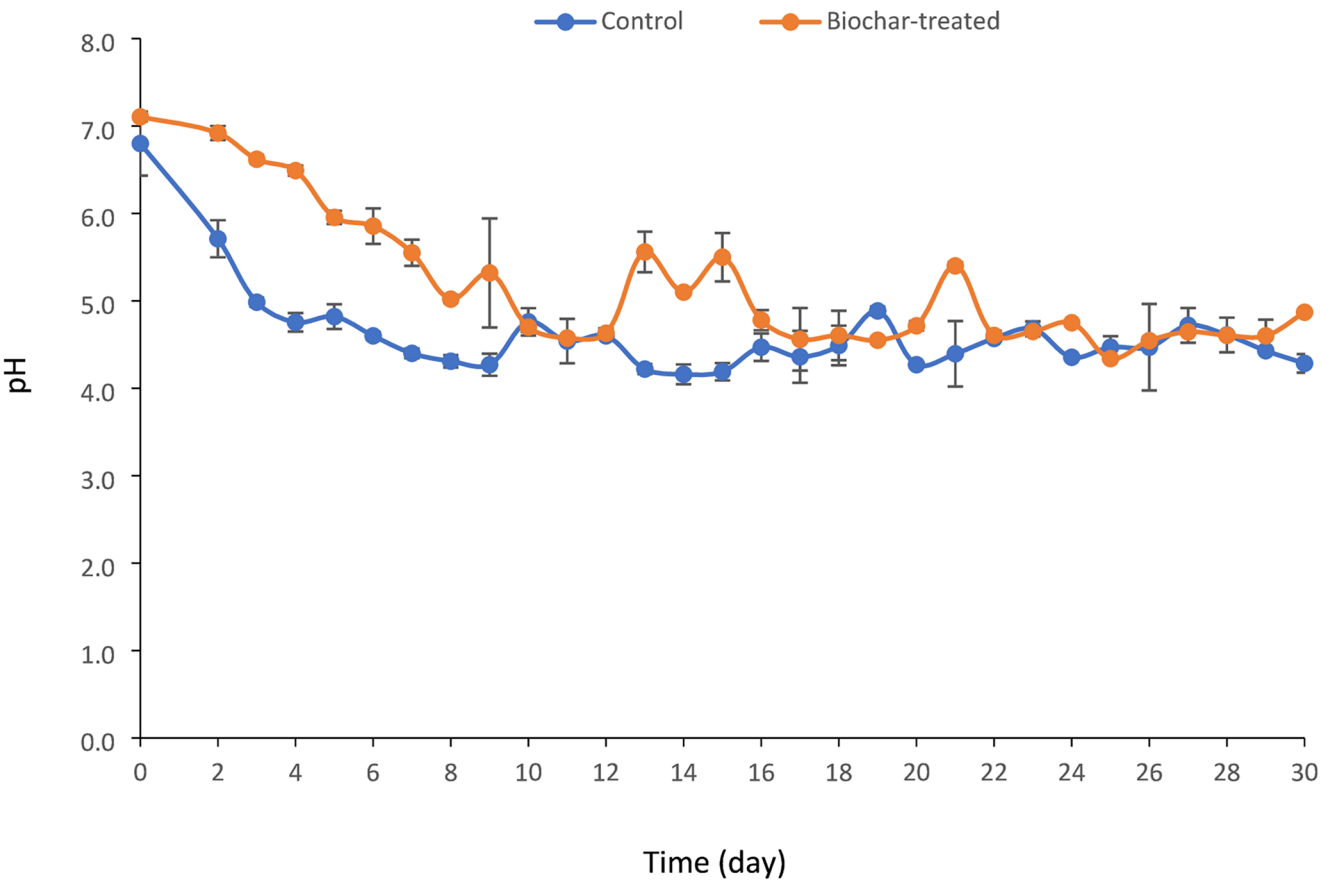

Fig. 6 pH variation in biochar-treated and non-treated (control) trials

Volatile Fatty Acid Composition

Figure 7 depicts the composition of VFAs obtained in control and biochar-treated experiments. Acetic acid was the prevalent VFA type in both experiments and a maximum acetic acid concentration of 15.23% (week 1) was obtained in the control experiment (Fig. 7A). The addition of biochar in the anaerobic digester improved the formation of VFAs as shown by the high acetic acid fraction of 53.23% in week 1 (Fig. 7B). The elevated VFA concentrations, specifically acetic acid, butyric acid, propionic acid, iso-valeric acid, and hexanoic acid, detected in the biochar-treated system are indicative of improved bioprocess efficiency. These byproducts serve as critical precursors in the methanogenesis phase of anaerobic digestion, as elucidated by Wu et al. [72]. Thus, a high concentration of these metabolites during the initial stages of anaerobic digestion is crucial for the successful endogenous fermentation of biogas and NPK-rich biodigestate. Sun et al. [73] observed that biochar improves the growth of the dominant VFA-producing acidogens, such as *Clostridium* species, leading to significant production of VFAs in the early phases of the anaerobic fermentation process. As anticipated, extending the anaerobic digestion period to week 4 resulted in a marked reduction in the formation of VFAs in both experimental setups (Figs. 7A and B). This decline can be attributed to the consumption of these intermediates by syntrophic fermentative microorganisms, including various archaeal communities [73]. A comparable pattern of VFA production and utilization was documented by Ding et al. [74] in an anaerobic digestion process that employed coconut-based biochar to enhance reactor performance. Meng et al. [75] discovered that biochar alleviates metabolic stress caused by VFAs by enhancing both their production and subsequent upgrading to biomethane, resulting in high yields.

Biodigestate Composition

This study also examined the anaerobic digestion system's capacity to produce biofertilizer by determining the concentration of nitrogen (N), phosphorus (P), and potassium (K) in the liquid phase of the anaerobic digestate (Table 5). In the control experiment, the N, P, and K contents were found to be 89.08 ± 0.23, 491.69 ± 2.60, and 3029.49 ± 0.56 mg/L, respectively. The addition of biochar in the biocatalytic digester had a positive effect on the composition of

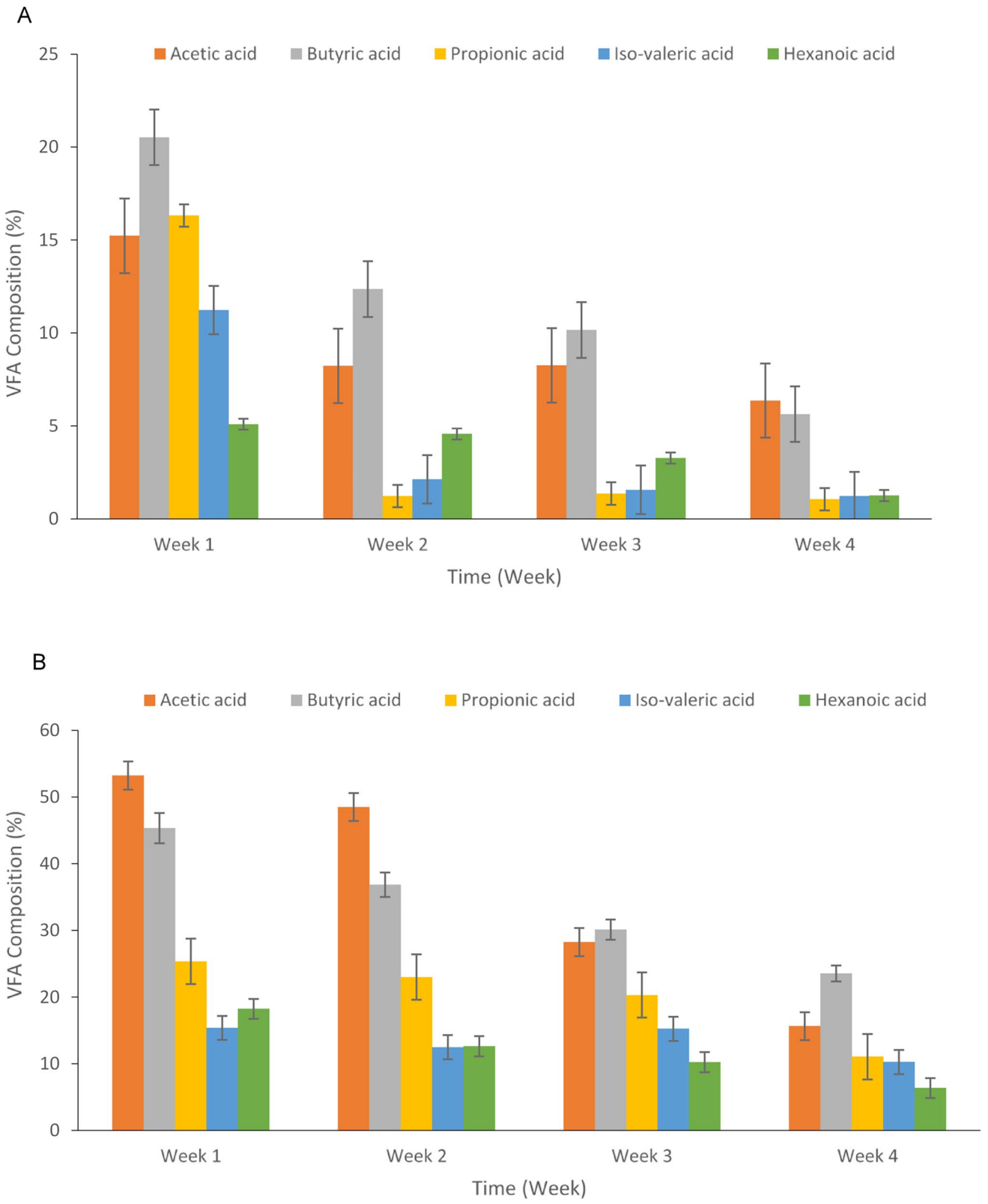

Fig. 7 VFA composition for the control (**A**) and biochar-treated (**B**) experiment

Table 5 NPK and micro/macro-nutrients in the biodigestate

Biodigestate content (mg/L)	Control	Biochar-treated
Nitrogen (N)	89.8 ± 0.23	92.12 ± 0.13
Phosphorus (P)	491.69 ± 2.60	682.08 ± 0.21
Potassium (K)	3029.49 ± 0.56	4238.06 ± 0.05
Ca	193.54 ± 0.37	186.21 ± 0.98
Mg	2690. 00 ± 0.45	2823.03 ± 0.13
Fe	14770.00 ± 2.10	2012.23 ± 0.62
B	1858.40 ± 0.89	1685.23 ± 0.75
Cu	147.60 ± 0.57	154.86 ± 0.55
Al	2170.00 ± 1.01	3201.56 ± 0.34
Zn	5612.20 ± 0.03	6571.25 ± 0.66
NH_4	114.72 ± 0.83	156.65 ± 0.85
S	48.40 ± 0.03	52.40 ± 0.46
NO_3	< 5.00	10.05 ± 0.17
NO_2	< 0.01	< 5.00
Mo	< 20	< 10

biodigestate as evidenced by the improved concentrations. Herein, the concentrations of N, P, and K were recorded as 92.12 ± 0.13, 682.08 ± 0.21, and 4238.06 ± 0.05 mg/L. It is worth highlighting that the underlying bioaugmentation mechanisms of biochar on NPK generation are not well elucidated in the literature. Nevertheless, a possible explanation for the observed phenomenon could be the functional groups and minerals found in the biochar, which improve the physical and chemical properties of the digestate, thus leading to the high bioavailability of NPK in the fermented effluent [75]. Moreover, the carbon-rich biochar (69.42%) observed in Table 1 creates optimal microenvironments for microbial growth and activity that lead to nutrient recycling processes and the bioavailability of NPK elements [75]. This is in line with a recent publication that reported that biochar-treated compost consists of high contents of NPK compared to non-treated soils due to enhanced biochemical activities [76]. Therefore, the recovery of nutrients from anaerobically digested biowaste streams presents an innovative digestate valorization approach that supports sustainable agronomic solutions, thereby reducing the high reliance on hazardous chemical fertilizers, in accordance with the emerging global circular bioeconomy principles.

Morphological Profile of Endogenous Inocula During Biocatalytic Trials

The ability of biochar to function as a biocarrier for the adsorption of biofilm-forming microorganisms is increasingly acknowledged within the scientific community [77–79]. Its exceptional functional properties, particularly its large surface area and porous structure, create microenvironments conducive to the colonization of microbes on its surface. This attachment leads to enhanced carbon assimilation, the development of exoelectrogenic microbes, increased defense against inhibitors, and improved recovery of final products [80, 81]. This was also observed in our study as the biochar possessed a high surface area of 140.29 m^2/g (Table 2) coupled with the porous honeycomb-like structures (Fig. 2), which aid in microbial colonization and biofilm formation (Fig. 8b). This also promotes syntrophic

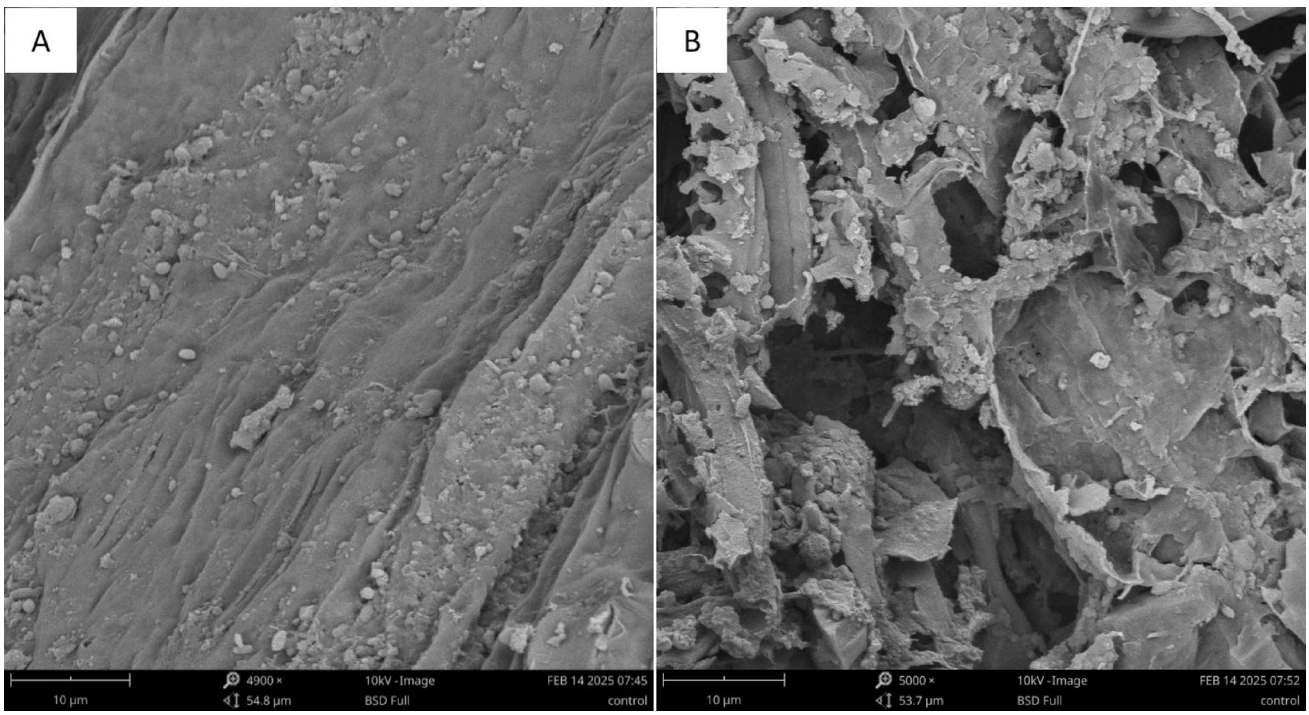

Fig. 8 SEM morphology for control (**A**) and biochar-treated (**B**) experiment

interactions among different microbial species, as observed by the abundance of the Pseudomonadota, in contrast to the non-treated system (Fig. 8a), which exhibited a smooth surface characterized by the dominance of planktonic cells.

A similar morphological pattern was documented by Tahsini et al. [81] in their characterization of the biofilm-forming communities in the biochar-mediated biocatalytic system utilized in the biotransformation of municipal solid waste. The authors also observed that biochar enhances the production of extracellular polymeric substances (EPS) within biofilm-forming microbial networks, a natural polymer that heterogeneous biofilm communities utilize to regulate their metabolic functions [81]. Therefore, the development of biochar-mediated biofilm fermenters will play an instrumental role in bioaugmenting the biocatalytic valorization of food waste as demonstrated in this study.

Carbon Assimilation and Cellulolytic Activity During Biocatalytic Trials

To determine how biochar affects the consumption of the carbon source by the fermentative microorganisms, the carbohydrate utilization in the control and biochar-treated experiments was measured using HPLC as shown in Fig. 9. The initial carbohydrate concentration decreased steadily within the 30 day anaerobic fermentation process from 65 g/L to 8.78 g/L and 65 g/L to 4.07 g/L for the control and the biochar-treated experiment, respectively (Fig. 9). The high carbon consumption observed in the biochar-treated bioprocess is due to the bioaugmentation of synergistic multi-step carbohydrate-driven metabolisms associated with the biocatalytic conversion of food waste. Also, adding biochar improves the microbial carbon conversion kinetics of the growth nutrients as reported by Valentin and Białowiec [82] in a study that explored carbon assimilation in biochar-treated and non-treated bioreactors during fermentation.

To further substantiate these findings, an additional step was taken to gain fundamental insights into the hydrolytic conversion of food waste into its final biobased products by examining the cellulolytic enzyme activity during the fermentation trials (Fig. 10). Compared to the control, the biochar-treated bioprocess demonstrated high cellulolytic activity. In this case, the cellulolytic activity decreased steadily from 0.82 to 0.32 nmol μl^{-1} min^{-1} per 100 mg of food waste, whereas the control showed a decline from 0.66 to 0.20 nmol μl^{-1} min^{-1} over the same digestion period. The decrease observed in both setups is likely attributed to substrate depletion, specifically food waste [11]. This fermentation step is regulated by dominant hydrolytic species such as *Bacillus* and *Clostridium* [11].

Microbial Community Analyses

Microbial Diversity and Sequencing Quality

High-throughput 16 S rRNA gene amplicon sequencing revealed significant differences in microbial recovery and community composition in biochar-amended anaerobic co-digestion systems compared to controls. Biochar treatment yielded 2,541 high-quality sequences (accuracy> QV40), 4.5-fold increase over the 568 sequences obtained in the control system (Fig. 11a). Post-quality filtering *via* the DADA2 pipeline, 71.50% of biochar sequences were taxonomically assignable compared to only 23.40% in the control (Fig.

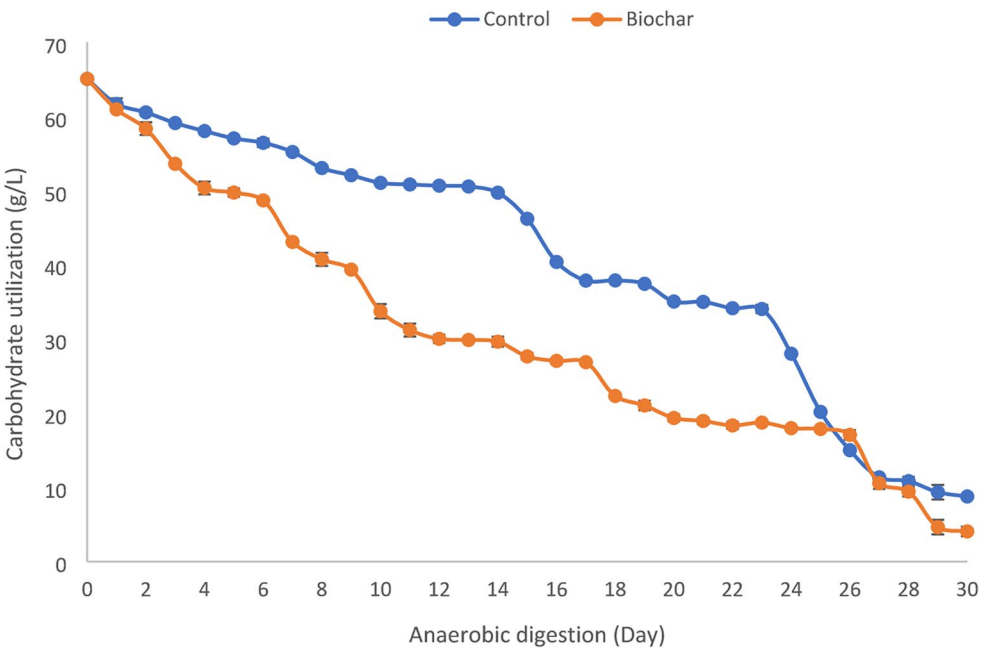

Fig. 9 Carbohydrate consumption in control (**A**) and biochar-treated (**B**) experiment

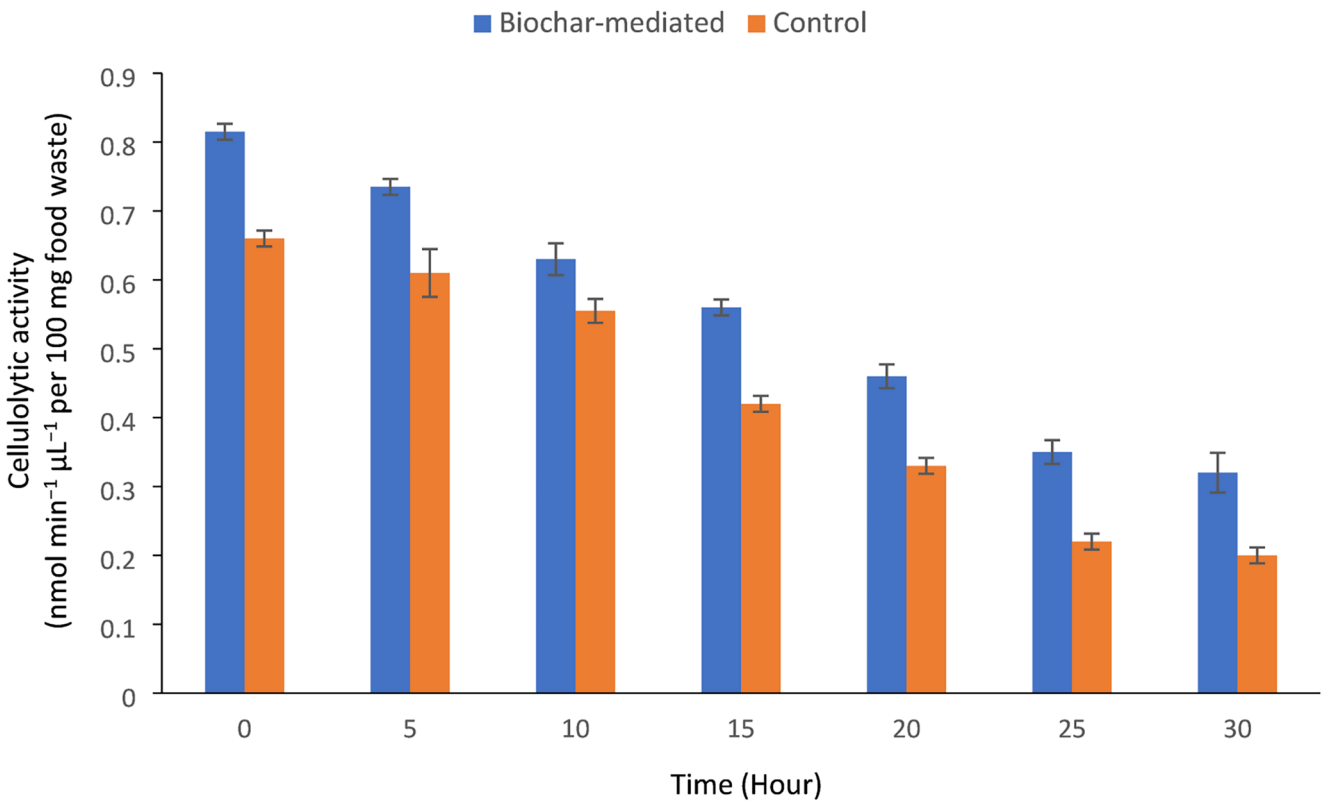

Fig. 10 Cellulolytic activity in biochar-treated and control trials

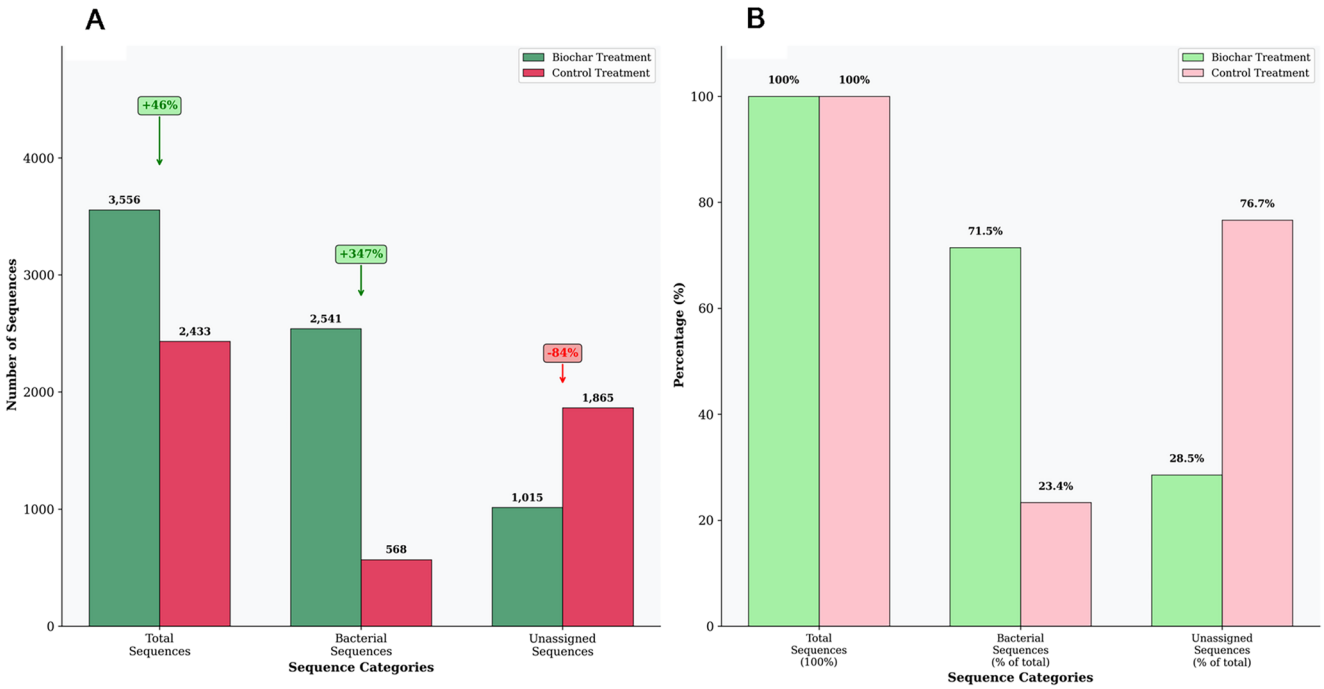

Fig. 11 Sequencing quality (**A**) and community composition (**B**) in both the biochar and control treatments during anaerobic food waste valorization

11b), suggesting biochar enhances DNA preservation and selectively enriches well-characterized bacterial lineages [83, 84]. This effect is likely attributable to biochar's porous structure and surface adsorption properties, which help protect microbial biomass and DNA from degradation [85]. However, as observed in Fig. 11b, the unassigned sequences dominated the control (76.6%) as compared to only 28.5% of biochar sequences that could be linked to the presence of novel taxa [86, 87].

At the phylum level, biochar amendment shifted the community to a dual dominance of two phyla with *Pseudomonadota* accounting for 48.76% (n = 1,239 abundance sequence) and *Bacteroidota* 25.23% (n = 641 abundance sequence), which collectively represent 73.99% of the bacterial community (Fig. 12a). In contrast, the control treatment system were co-dominated by *Pseudomonadota* at 42.25% (n = 240 abundance sequence) and Campylobacterota at 25.00% (n = 142) (Fig. 12b). This pronounced shift indicates biochar imposes selective pressures favouring metabolically versatile taxa with key functional roles in nutrient cycling and organic matter degradation [88–90].

Functional Guild Distribution

Genus-level analysis highlighted functional specialization with implications for biocommodity production (Table 6 and Supplementary Figure S1a and b). Table 6 summarizes key genera such as *Comamonas*, *Bacteroides* I, *Aliarcobacter*, and *Romboutsia*, along with their relative abundances, enrichment factors, and primary functions. These taxa exhibited distinct responses to biochar amendment, reflecting shifts in ecological niches and metabolic contributions that support process stability, nutrient recovery, and substrate conversion efficiency. *Comamonas*, a phosphate-solubilizing genus, reached 25.54% abundance in the biochar treatment, a 2.5-fold enrichment over controls (10.21%). This enrichment correlated with enhanced phosphorus recovery in biochar-derived biofertilizers (682.08 mg/L compared to 491.69 mg/L in the control). Phosphate solubilization by *Comamonas* is mediated by key genes such as *gcd* (encoding quinoprotein glucose dehydrogenase) and *glp* (involved in glycerol-3-phosphate pathways), which facilitate the release of orthophosphate from insoluble forms; in biochar-amended systems, the provision of conductive surfaces and microelements (iron) likely promotes *Comamonas* as a syntrophic partner, aligning with observed improvements in phosphorus transformation and availability [91–93]. *Bacteroides*, associated with cellulolytic activity, increased to 11.22% in the biochar system from 5.99% in the control, supporting improved residual carbohydrate utilization (from initial 65 to 4.07 g/L in biochar compared with 8.78 g/L in the control). Cellulolytic activity in *Bacteroides* is driven by diverse glycoside hydrolase (GH) families that hydrolyze complex polysaccharides, including cellulose, thereby enhancing hydrolysis and acidogenesis stages. Biochar amendment selectively enriches such hydrolytic taxa, facilitating the breakdown of refractory organics and contributing to elevated volatile fatty acid production for subsequent

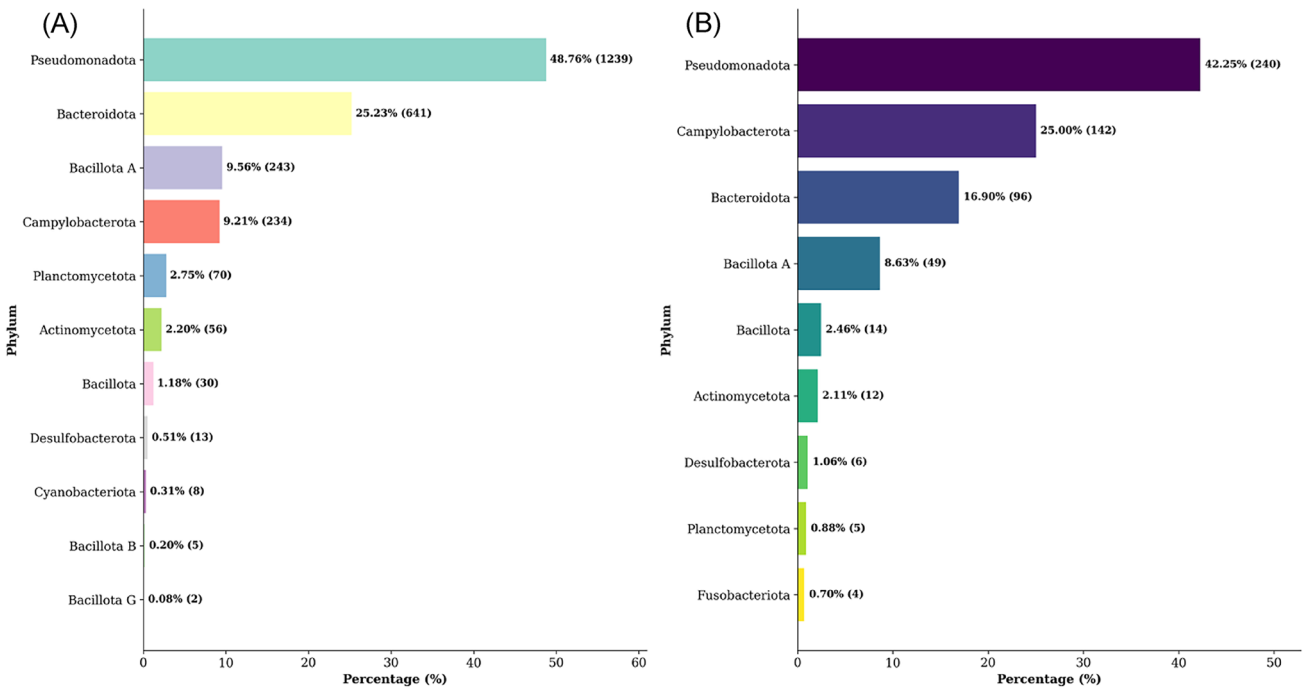

Fig. 12 The Phylum distribution in biochar (**A**) and control (**B**) treatments during anaerobic food waste valorization

Table 6 Key bacterial genera and their functional roles in biochar-amended and control in anaerobic co-digestion systems

Genus	Relative abundance in biochar (%)	Relative abundance in control (%)	Enrichment compared to control	Primary function	Reference
Comamonas	25.54	10.21	Substantially higher in biochar (2.5×)	Phosphate solubilization; correlated with enhanced P recovery in biochar systems (facilitated by *gcd/glp* genes encoding glucose/glycerol-3-phosphate dehydrogenases for orthophosphate release).	[96]
Bacteroides I	11.22	5.99	Higher in biochar (1.9×)	Cellulose degradation; cellulolytic/CAZyme potential (glycoside hydrolase families) supporting improved carbohydrate turnover and hydrolysis in complex organic matrices.	[97]
Aliarcobacter	9.26	25.18	Lower in biochar	Organic acid production, reduced abundance suggests altered acidogenic dynamics and VFA patterns (fermentative contributions to acetate and other acids in anaerobic consortia).	[98]
Romboutsia	6.49	4.96	Slightly higher in biochar (1.3×)	Acetogenesis; associated with acetic acid production and DIET-linked acetogenic roles (facilitating intermediate metabolite stabilization and syntrophic acetate supply).	[99]

methanogenesis [94]. Conversely, *Aliarcobacter* exhibited lower abundance in the biochar treatment (9.26% against 25.18% in control), potentially reflecting niche displacement under conditions favoring more efficient syntrophs or reduced acid stress. This genus contributes to organic acid production, including acetate and other volatile fatty acids, through fermentative metabolism; although less dominant in biochar systems, its presence in controls underscores its role in acidogenic consortia, with biochar potentially shifting fermentation patterns toward stabilized intermediates [94]. *Romboutsia* showed slightly higher abundance in biochar (6.49% compared to 4.96% in control), consistent with its involvement in acetogenic metabolism. *Romboutsia* participates in acetogenesis, producing acetic acid and supporting syntrophic interactions, often enhanced by biochar's promotion of direct interspecies electron transfer (DIET). This genus contributes to intermediate metabolite degradation and acetate supply, aiding methanogenic stability in wood-derived or similar biochar amendments [95]. Eight genera were shared across treatments, forming the functional core of anaerobic digestion, while biochar and control tests supported 23 and 25 unique genera, respectively, indicating distinct ecological niches shaped by biochar's unique properties (surface area, conductivity, and nutrient retention). These community shifts underpin improved process performance, including higher phosphorus recovery for biofertilizer applications and enhanced carbohydrate degradation for biogas yield.

Species-Level Functional Specialization

At the species level, *Comamonas avium* dominated biochar systems at 25.05% (n = 633 abundance sequence), comprising 97.53% of *Comamonas* sequences and driving enhanced phosphorus mobilization (Fig. 13a). In contrast, *Aliarcobacter suis* was prevalent in the control (Fig. 13b) at 25.18% (n = 142 abundance sequence) but reduced to 9.26% (n = 234 abundance sequence) in biochar treatments, suggesting suppression of potentially undesirable taxa [100–102]. Core acetogenic species, such as *Romboutsia* sp. 018336475, maintained stable abundance (6.49% in biochar compared to 4.96% in controls), preserving volatile fatty acid (VFA) production pathways [103]. Generally, the biochar systems hosted 39 unique species compared with the 26 species of the control, and 9 were shared, highlighting treatment-specific functional specialization [104].

Microbial Diversity and Ecosystem Stability

Biochar-amended systems showed significantly higher alpha diversity compared to the control treatment (Table 7). Shannon diversity increased by 27.5% in biochar treatments ($H' = 3.45 \pm 0.11$) compared to controls ($H' = 2.71 \pm 0.04$; p = 0.012), indicating greater species evenness and niche partitioning. This enhancement is attributed to biochar's heterogeneous microenvironments, which promote niche availability and reduce competitive exclusion *via* its porous architecture and ion exchange capacity [105]. A similar

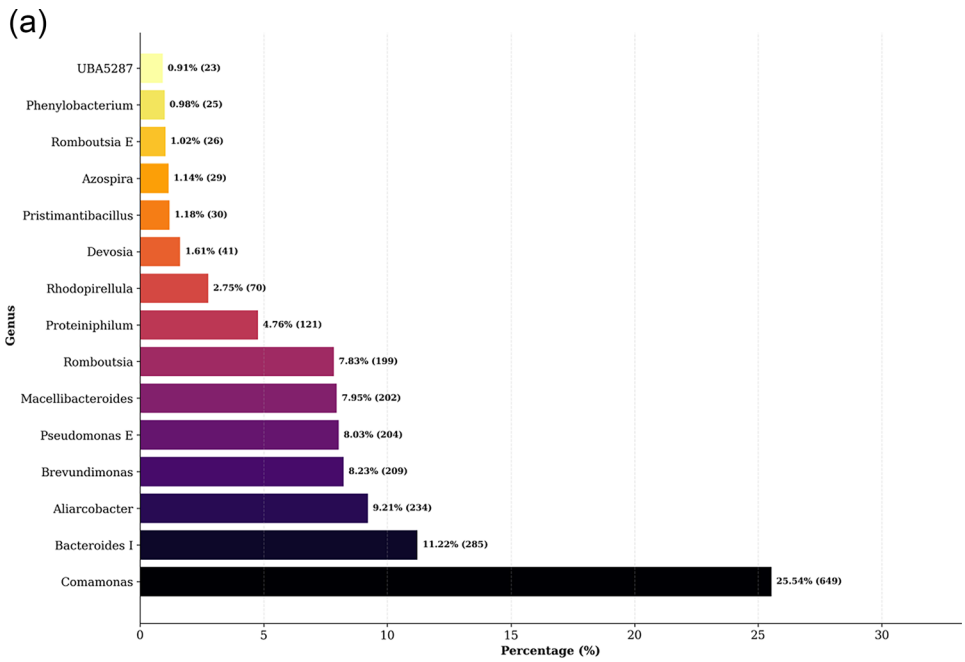

Fig. 13 Species-level taxonomic distribution of biochar (**A**) and control (**B**) treatment obtained during anaerobic food waste valorization

pattern emerged from the Simpson diversity (1-D), which increased from 0.83 ± 0.004 in control to 0.87 ± 0.011 in biochar- amended systems (p = 0.041), reflecting reduced species dominance and more equitable resource distribution. Although Chao1 richness was estimated at 156 ± 11.0 species in the biochar system versus 143 ± 4.00 in the control, the difference was not statistically significant (p = 0.078). This observation reflects modest enhancement of rare taxa with specialized metabolic roles.

Conversely, beta diversity analysis using Bray-Curtis dissimilarity revealed no significant difference in overall community composition between treatments (mean dissimilarity = 0.694 at p = 0.330; Table 7). These results indicate that biochar primarily enhances within-sample microbial diversity through greater evenness and modest increases in richness, without substantially restructuring community structure. Biochar thus appears to act as a primary driver of community assembly, creating distinct selective environments that reshape microbial communities toward biocommodity-enhancing configurations.

Nutrient Transformation Networks

Biochar amendment enriched phosphate-solubilizing bacteria (*Comamonas*, *Pseudomonas*, and *Brevundimonas*), which comprised 41.8% of the biochar community compared to 24.66% in the control treatment, supporting a 38.8% increase in phosphorus recovery (693.7 mg/L vs. 587.2 mg/L) (Fig. 14A). These findings align with prior biochar studies in anaerobic co-digestion systems, demonstrating consistent enhancements in nutrient cycling [106, 107]. Cellulolytic guilds, dominated by *Clostridium*, further decreased from 90.9% in the control to 83.7% in biochar systems, with a compensatory increase in *Bacteroides* (5.99% to 11.22%), ensuring balanced hydrolytic activity without setbacks (Fig. 14B). Fermentative *Bacillota* remained stable (11% in both treatments), preserving organic acid production pathways that are critical for nutrient cycling (Fig. 14B) [108]. The parallel rise in *Comamonas* abundance (14.7% to 25.5%) and phosphorus recovery (Fig. 14C) underscores biochar's role in enhancing polyphosphate accumulation and nutrient assimilation [109]. Nutrient-transforming guilds showed reduced *Clostridium* (55.3% to 41.6%) and increased *Pseudomonas* (11.1% to 20.4%), *Comamonas* (10.1% to 16.5%), and *Acinetobacter* (5.0% to 10.6%) in biochar systems (Fig. 14D), reflecting a shift toward multifunctional communities that sustain nutrient turnover and system resilience [110]. These microbial shifts also support improved biogas production through stabilized fermentation pathways, which demonstrate biochar's capacity to optimize microbial communities for improved resource recovery and biochemical stability in anaerobic co-digestion systems, with potential implications for integrated biogas-biofertilizer production technologies.

Techno-Economics of a Biochar-Mediated Bioprocess

To acquire insights into the economic feasibility of establishing a biochar-mediated system tailored for anaerobic digestion, where biogas and biofertilizer are the main products, a preliminary techno-economic (TEA) study was undertaken. Such an assessment provides critical economic insights that can guide the development, optimization, and

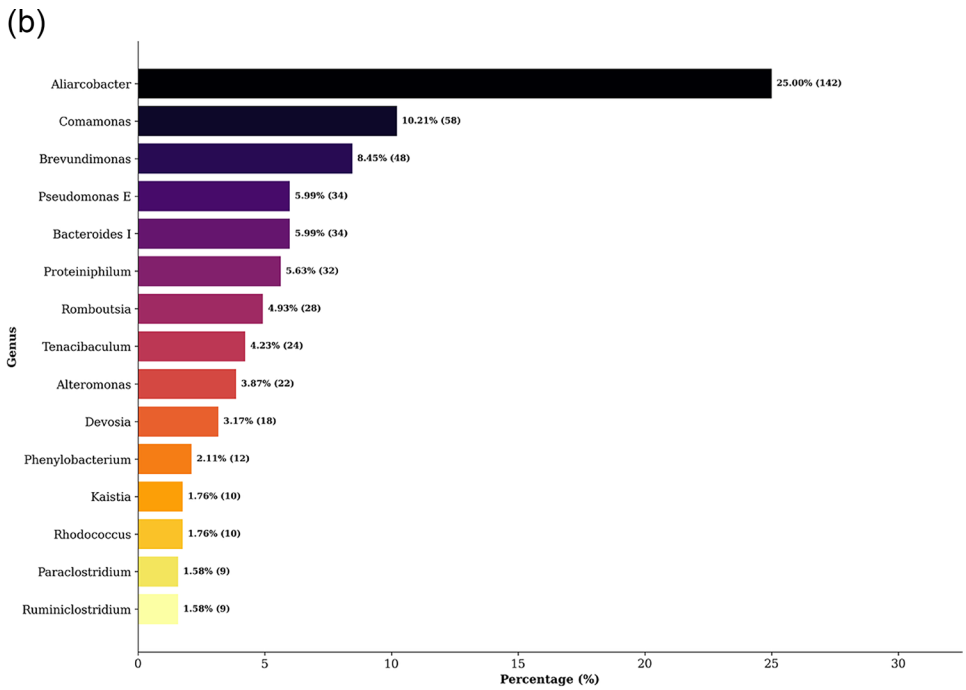

Fig. 13 (continued)

Table 7 Key bacterial genera and their functional roles in biochar-amended and control during anaerobic co-digestion processes

Diversity Index	Metric	Biochar	Control	*p*-value
Alpha	Shannon Index (H′)	3.450 ± 0.110	2.710 ± 0.040	0.012*
	Simpson Index (1-D)	0.870 ± 0.011	0.830 ± 0.004	0.041*
	Chao1	156.0 ± 11.00	143.0 ± 0.400	0.078 ns
Beta	Bray-Curtis dissimilarity	0.694		0.330ns

Values are mean ± SD for alpha diversity. *Indicates significance at $P \leq 0.05$ (Benjamini–Hochberg (BH) adjusted). Beta diversity was tested with PERMANOVA

future scale-up of biorefineries. In this study, a profitability analysis approach was applied to estimate the potential economic performance of the process.

The primary operating cost components include raw materials such as distilled water, food waste, and biochar, which are summarized in Table 8. For this assessment, food waste is assumed to be obtained at no cost from nearby food waste suppliers, reflecting common waste diversion/valorization practices where biodegradable waste residues are provided free of charge to treatment facilities. Consequently, transportation costs were considered negligible due to the proximity of the waste source to the production site.

The process operates in a batch mode over 720 h (30 days), representing a typical anaerobic digestion cycle for the co-production of biofertilizer and biogas. To simplify the analysis, biochar derived from *Eucalyptus grandis* wood is assumed to be externally sourced at a fixed market price of R50 kg^{-1}. Therefore, the capital costs associated with biochar production via slow pyrolysis are excluded from this preliminary assessment.

As shown in Table 8, a large fraction of the projected revenue is obtained from biofertilizer, primarily due to its higher market value and production yield compared with biogas. The integration of biochar into the anaerobic system enhances microbial activity and nutrient retention, which can improve the quality and agronomic value of the resulting digestate, thereby strengthening its commercial potential as a biofertilizer. These findings highlight the economic promise of biochar-induced anaerobic bioprocesses as a sustainable strategy for resource recovery from food waste within circular bioeconomy frameworks.

Table 9 shows the total operating cost and the profitability of the process with and without labor. The process is characterized by zero-energy cost with minimal labour requirements. The labour cost, while minimal, dominates the operating cost. The labour process is only required during the preparation, loading, start-up, monitoring (< 30 min per day), analysis of results, and shutdown. This is approximated to take a total of 5 h in the overall 30 day operation cycle. Only one technician billed at R650/hour is needed, with no shift changes necessary. The process generates a total profit of R159 384,16 as presented in Table 9. The total operating cost (incl. labour cost) takes about 2.21% of the entire cost flow. This indicates that the biochar-mediated

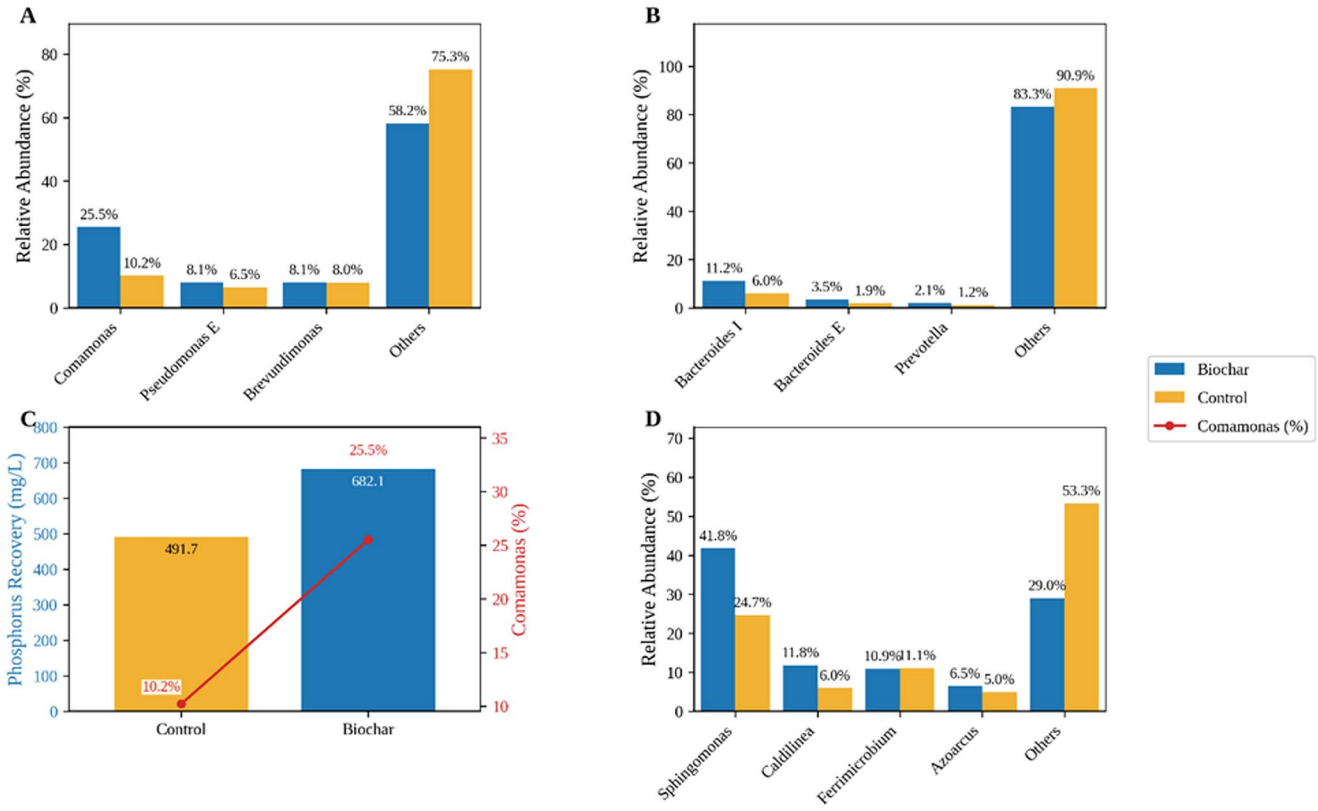

Fig. 14 Functional guild distribution and nutrient transformation networks distribution of bacterial genera in biochar and control treatment obtained from an anaerobic co-digestion system. **A** phosphate-solubilizing bacteria **B** cellulolytic bacteria, **C** phosphorus recovery against *Comamonas* Abundance, and **D** relative abundance of nutrient transformation

Table 8 Raw and product materials, and their associated costs

Batch capacity	1000 L			
Raw Materials	Price (*R*/kg)	% Usage per batch	Mass usage per batch (kg)	Price per batch (*R*)
Distilled water	0,04	229,51	700	28
Food waste (kg)	0	81,97	250	0
Biochar (kg)	50	1,64	5	250
Main Products	**Price**	**Density**	**Capacity**	**Sales**
Biofertilizer	R 60/L	1.11 kg/L	100 kg/day	R162 162,16
Biogas	R 40/kg	1.25 kg/m3	500 L/day	R 750, 00

Table 9 Profitability analysis of the biochar-mediated process for biofertilizer and biogas

Total operating cost (Incl. Labour)	*R* 3 528,00
Total operating cost (Excl. Labour)	R 278,00
Profit (Excl. Labour)	R 162 634,16
Total Profit (Incl. Labour)	**R 159 384,16**

process is attractive for investment and further scale-up. Future work should focus on the scale-up of the process to commercial scale, with consideration of the upstream biochar production process scale-up and investment. Comparison between fast and slow pyrolysis will determine the final selling price of biochar as a valuable commodity.

Compared with other commonly used bio-additives, biochar demonstrates a competitive cost advantage. For example, activated carbon, which is widely utilized as an adsorbent and microbial support material, is reported to cost R24 – R33 kg^{-1} in South African markets [111], with international prices ranging from $1,500 – $2,700/ton, depending on grade and specification [112]. In contrast, the biochar applied in this study was assumed to have a purchase price of R50 kg^{-1}. This cost is considered economically reasonable, particularly given that biochar can be locally produced from copious lignocellulosic wastes such as *Eucalyptus grandis* and does not require the high-temperature activation processes necessary for activated carbon production. Therefore, biochar represents a cost-effective alternative

bio-additive for anaerobic-based biorefinery systems, while retaining beneficial properties such as high surface area, porosity, and functional groups that facilitate microbial attachment and enhance process stability [113].

Limitations, Recommendations, and Future Research

In spite of the promising results observed in this work, there are a lot of significant knowledge gaps that must be addressed to obtain in-depth insights into the bioaugmentation effects of biochar-mediated closed-loop food valorization biorefinery scenarios. The main bottleneck of the current study is its narrow feedstock scope, as only fruit and vegetable waste was evaluated. Therefore, future research should incorporate protein- and fat-rich food waste residues to improve the extensibility of the outcomes and better reflect practical (real-world) food waste management scenarios. Also, it is important to examine different biomass sources for biochar production, as the chemical composition, including lignin, hemicellulose, and cellulose, significantly affects the final physicochemical properties and functional role of the manufactured biochar.

Another significant research gap is the lack of understanding regarding optimal biochar-producing conditions, including the biomass fractionation temperature, retention time, and heating rate, which directly affect the desirable surface properties and functional groups. The application of multivariate optimization tools could provide invaluable insights in this domain. Additionally, the mechanistic basis of biochar-mediated enrichment in food waste valorization studies remains scantily elucidated. Future work should leverage advanced molecular tools, such as OMICS technologies, to investigate the individual and synergistic microbial and biochemical mechanisms governing this bioprocess.

Further research should also explore the long-term stability and reusability of biochar, for example, over multiple digestion cycles, and examine the potential benefits of biochar modification, such as nutrient doping, to enhance its performance. The role of biomass origin and regional conditions, particularly for forestry-derived feedstocks, should be systematically evaluated, given their impact on biochar properties. Finally, integrating TEA assessments and life-cycle analyses (LCA) of the entire "woodchip → biochar → food waste valorization" chain is crucial to generate data that can guide the scale-up, optimization, and sustainability assessment of pilot- and industrial-scale biorefineries.

Conclusion

This study elucidates the transformative role of *Eucalyptus grandis*-derived biochar in enhancing food waste valorization through pilot-scale anaerobic co-digestion. The biochar's physicochemical properties, including a high surface area (140.29 m^2/g), mesoporous structure (2.0 nm), and diverse functional groups, confirmed by SEM, BET, CHNS, FTIR, TGA, and XRD, facilitated significant bioaugmentation. Biochar amendment stabilized pH (7.06–5.50 compared to 4.37 in the control), increased volatile fatty acid production (53.23% acetic acid relative to 15.23% in the control), and improved nutrient recovery, yielding biofertilizer with enhanced NPK content (92.12, 682.08, and 4238.06 mg/L for N, P, and K, respectively), including a 38.8% increase in phosphorus recovery. Microbial community restructuring enriched phosphate-solubilizing bacteria (41.8% compared to 24.66% in the control) and improved taxonomic assignability (71.46% relative to 23.35%), enhancing process stability. These findings position biochar-mediated anaerobic process as an innovative and cost-effective strategy for food waste valorization, advancing circular bioeconomy principles and sustainable waste management in developing regions. By integrating pH stability, VFA production, nutrient recovery, and microbial optimization, this approach provides a scalable framework for biorefinery development, contributing to the UN's Sustainable Development Goals 2 (Zero Hunger), 12 (Responsible Consumption and Production), and 13 (Climate Action).

Supplementary Information The online version contains supplementary material available at https://doi.org/10.1007/s12649-026-03686-w.

Funding Open access funding provided by North-West University.

References

1. Patel, A., Sarkar, O., Rova, U., Christakopoulos, P., Matsakas, L.: Valorization of volatile fatty acids derived from low-cost organic waste for lipogenesis in oleaginous microorganisms – A review.

Bioresour Technol. **321**, 124457 (2021). https://doi.org/10.1016/j.biortech.2020.124457
2. Nhleko, L., Sekoai, P.T.: Sugarcane Bagasse: A Sustainable Feedstock for Biorefinery Portfolios in South Africa. Fermentation. **11**, 489 (2025). https://doi.org/10.3390/fermentation11090489
3. European Commission: (2025). https://environment.ec.europa.eu/topics/circular-economy_en. Accessed 10
4. BBC: Climate change - EU leaders set 55% target for CO_2 emissions cut. (2025). https://www.bbc.com/news/world-europe-55273004. Accessed 10
5. Hackula, A., O'Shea, R., Murphy, J.D., Wall, D.M.: Developing distillery biorefineries through dark fermentation of whiskey production by-products: the effect of organic loading rate on decarbonisation pathways. Energy Conv Man. **301**, 118064 (2024). https://doi.org/10.1016/j.enconman.2024.118064
6. Sekoai, P.T., Chunilall, V., Msele, K., Habimana, O., Swartbooi, A., Johakimu, J., et al.: Biowaste biorefineries in South Africa: Current status, opportunities, and research and development needs. Ren. Sustain. Energy Rev. **188**, 113870 (2023). https://doi.org/10.1016/j.rser.2023.113870
7. Martínez-Mendoza, L.J., Muñoz, R., García-Depraect, O.: Continuous Fermentative Biohydrogen Production from Fruit-Vegetable Waste: A Parallel Approach to Assess Process Reproducibility. Fermentation. **11**, 545 (2025). https://doi.org/10.3390/fermentation11090545
8. Dou, Z., Toth, J.D.: Global primary data on consumer food waste: Rate and characteristics – A review. Resour. Cons Recyc. **168**, 105332 (2021). https://doi.org/10.1016/j.resconrec.2020.105332
9. Sekoai, P.T., Roets-Dlamini, Y., O'Brien, F., Ramchuran, S., Chunilall, V.: Valorization of Food Waste into Single-Cell Protein: An Innovative Technological Strategy for Sustainable Protein Production. Microorganisms. **12**, 166 (2024). https://doi.org/10.3390/microorganisms12010166
10. Callejas, C., López, I., Bovio-Winkler, P., Etchebehere, C., Borzacconi, L.: Temporal analysis of the microbiota involved in the anaerobic degradation of sugarcane vinasse in a full-scale methanogenic UASB reactor. Biomass Conv Bioref. **12**, 3887–3897 (2022). https://doi.org/10.1007/s13399-021-01281-8
11. Srinivas, M., O'Sullivan, O., Cotter, P.D., Sinderen, D., Kenny, J.G.: The Application of Metagenomics to Study Microbial Communities and Develop Desirable Traits in Fermented Foods. Foods. **11**, 3297 (2022). https://doi.org/10.3390/foods11203297
12. Fan, L., Peng, W., Duan, H., Lü, F., Zhang, H., He, P.: Presence and role of viruses in anaerobic digestion of food waste under environmental variability. Microbiome. **11**, 170 (2023). https://doi.org/10.1186/s40168-023-01585-z
13. Areniello, M., Matassa, S., Esposito, G., Lens, P.N.L.: Biowaste upcycling into second-generation microbial protein through mixed-culture fermentation. Trends Biotechnol. **41**, 197–213 (2023). https://doi.org/10.1016/j.tibtech.2022.07.008
14. Hale, L., Luth, M., Crowley, D.: Biochar characteristics relate to its utility as an alternative soil inoculum carrier to peat and vermiculite. Soil. Biol. Biochem. **81**, 228–235 (2015). https://doi.org/10.1016/j.soilbio.2014.11.023
15. Velasquez-Pinas, J.A., Ghofrani-Isfahani, P., Maya, D.Y., Costa, J.M., Forster-Carneiro, T., Angeliki, I.: Understanding the effect of biochar characteristics on anaerobic digestion with focus in food processing industry. Biomass Bioenergy. **201**, 108154 (2025). https://doi.org/10.1016/j.biombioe.2025.108154
16. Stafford, W., De Lange, W., Nahman, A., Chunilall, V., Andrew, J., Johakimu, J., Sithole, B., et al.: Forestry biorefineries. Renew. Energy. **154**, 461–475 (2020). https://doi.org/10.1016/j.renene.2020.02.002
17. Crafford, P.L., Wessels, C.B.: South African log resource availability and potential environmental impact of timber construction. South. Afr. J. Sci. **116**, 6419 (2020). https://doi.org/10.17159/sajs.2020/6419
18. Hirsch, H., Allsopp, M.H., Canavan, S., Cheek, M., Geerts, S., Geldenhuys, C.J., Harding, G., et al.: *Eucalyptus camaldulensis* in South Africa – past, present, future. Trans. Royal Soc. South. Afr. **75**, 1–22 (2020). https://doi.org/10.1080/0035919X.2019.1669732
19. Chicaiza-Ortiz, C., Zhang, P., Zhang, J., Zhang, T., Yang, Q., He, Y.: CO_2-enhanced methane production by integration of bamboo biochar during anaerobic co-digestion. J. Environ. Man. **373**, 123603 (2025). https://doi.org/10.1016/j.jenvman.2024.123603
20. Li, J., Qiu, C., Liu, N., Qi, L., Chen, X., Zhang, Y., et al.: Impact of biochar prepared at different pyrolysis temperatures on the methane production and microbial community structure of food waste anaerobic digestion. Int. J. Hydrogen Energy. **96**, 860–869 (2024). https://doi.org/10.1016/j.ijhydene.2024.11.335
21. Jiang, Q., Zhu, Q., Meng, Y., Huang, T., Liu, H.: Role and significance of nitrogen and sulfur-doping on algal biochar for regulating methane production. J. Water Process. Eng. **67**, 106123 (2024). https://doi.org/10.1016/j.jwpe.2024.106123
22. Fardi, Z., Shahbeik, H., Nosrati, M., Motamedian, E., Tabatabaei, M., Aghbashlo, M.: Waste-to-energy: Co-pyrolysis of potato peel and macroalgae for biofuels and biochemicals. Environ. Res. **242**, 117614 (2024). https://doi.org/10.1016/j.envres.2023.117614
23. Feng, K., Ansari, A.J., Zhang, N., Peng, Y., Song, X.: Biochar addition to mitigate oil inhibition in anaerobic digestion of food wastewater: Microbial insights from biochemical methane potential tests. Environ. Technol. Inn. **37**, 104000 (2025). https://doi.org/10.1016/j.eti.2024.104000
24. Ouyang, Y., Liu, Y., Tian, L., Ding, Y., Fan, G., Pan, C., et al.: Lipase pretreatment enhances biochar-assisted anaerobic digestion of food waste. Biofuels Biop Bioref. **19**, 189–205 (2025). https://doi.org/10.1002/bbb.2705
25. Lou, T., Yin, Y., Wang, J.: Improved production of medium-chain fatty acids by biochar: Effect of biochar dosage and mechanism. J. Clean. Prod. **450**, 14205 (2024). https://doi.org/10.1016/j.jclepro.2024.142051
26. Wu, J., Dong, L., Zhou, C., Liu, B., Xing, D., Feng, L., et al.: Enhanced butanol-hydrogen coproduction by *Clostridium beijerinckii* with biochar as cell's carrier. Bioresour Technol. **294**, 122141 (2019). https://doi.org/10.1016/j.biortech.2019.122141
27. Zhang, H., Voroney, R.P., Price, G.W.: Effects of temperature and processing conditions on biochar chemical properties and their influence on soil C and N transformations. Soil. Biol. Biochem. **83**, 19–28 (2015). https://doi.org/10.1016/j.soilbio.2015.01.006
28. Rorke, D.C.S., Lekha, P., Kana, G.E.B., Sithole, B.B.: Surfactant-assisted green liquor dregs pretreatment to enhance the digestibility of paper mill sludge. Int. J. Hydrogen Energy. **46**, 21359–21371 (2021). https://doi.org/10.1016/j.ijhydene.2021.04.018
29. Vandana, T.U., Tripathy, B.K., Mishra, R.K., Sharma, A., Mohanty, K.: A review on waste biomass-derived biochar: Production, characterisation, and advanced analytical techniques for pollutants assessment in water and wastewater. Process. Saf. Environ. Prot. **201**, 107505 (2025). https://doi.org/10.1016/j.psep.2025.107505
30. Jele, T.B., Sithole, B., Lekha, P., Andrew, J.: Characterisation of pulp and paper mill sludge for beneficiation. Cellulose. **29**, 4629–4643 (2022). https://doi.org/10.1007/s10570-022-04578-7
31. Zhang, Q., Niu, J., Guo, P., Wang, J., Peng, C., Zhang, et al.: Hydrolysis and methane yield enhancement of anaerobic co-digestion of kitchen waste and sewage sludge by air/carbon dioxide nanobubble water. Fuel. **381**, 133456 (2025). https://doi.org/10.1016/j.fuel.2024.133456
32. Li, Z., Jiang, X., Shi, W., Yang, D., Zhao, Y., Zhou, T.: Enhancement of Anaerobic Digestion from Food Waste via Ultrafine Wet Milling Pretreatment: Simulation, Performance, and Mechanisms.

Sustainability. **16**, 2933 (2024). https://doi.org/10.3390/su16072933
33. Gupta, K.K., Aneja, K.R., Rana, D.: Current status of cow dung as a bioresource for sustainable development. Bioresour Bioproc. **3**, 1–11 (2016). https://doi.org/10.1186/s40643-016-0105-9
34. Sekoai, P.T., Engelbrecht, N., du Preez, S.P., Bessarabov, D.: Thermophilic Biogas Upgrading via ex Situ Addition of H_2 and CO_2 Using Codigested Feedstocks of Cow Manure and the Organic Fraction of Solid Municipal Waste. ACS Omega. **5**, 17367–17376 (2020). https://doi.org/10.1021/acsomega.0c01725
35. Khayum, N., Anbarasu, S., Murugan, S.: Biogas potential from spent tea waste: A laboratory scale investigation of co-digestion with cow manure. Energy. **165**, 760–768 (2018). https://doi.org/10.1016/j.energy.2018.09.163
36. Rashidi, F., Kevlich, N.S., Sinquefield, S.A., Shofner, M.L., Nair, S.: Graphene Oxide Membranes in Extreme Operating Environments: Concentration of Kraft Black Liquor by Lignin Retention. ACS Sustain. Chem. Eng. **5**, 1002–1009 (2017). https://doi.org/10.1021/acssuschemeng.6b02321
37. Shen, J., Yan, H., Zhang, R., Liu, G., Chen, C.: Characterization and Methane Production of Different Nut Residue Wastes in Anaerobic Digestion. Renew. Energy. **116**, 835–884 (2018). https://doi.org/10.1016/j.renene.2017.09.018
38. Sahoo, S.S., Vijay, V.K., Chandra, R., Kumar, H.: Production and characterization of biochar produced from slow pyrolysis of pigeon pea stalk and bamboo. Clean. Eng. Technol. **3**, 10010 (2021). https://doi.org/10.1016/j.renene.2017.09.018
39. Yang, X., Wang, H., Strong, P.J., Xu, S., Liu, S., Lu, K., et al.: Thermal Properties of Biochars Derived from Waste Biomass Generated by Agricultural and Forestry Sectors. Energies. **10**, 469 (2017). https://doi.org/10.3390/en10040469
40. Veksha, A., McLaughlin, H., Layzell, D.B., Hill, J.M.: Pyrolysis of wood to biochar: increasing yield while maintaining microporosity. Bioresour Technol. **153**, 173–179 (2014). https://doi.org/10.1016/j.biortech.2013.11.082
41. Li, Y., Gupta, R., Zhang, Q., You, S.: Review of biochar production via crop residue pyrolysis: Development and perspectives. Bioresour Technol. **369**, 128423 (2023). https://doi.org/10.1016/j.biortech.2022.128423
42. Alghashm, S., Song, L., Liu, L., Ouyang, C., Zhou, J.L., Li, X.: Improvement of Biogas Production Using Biochar from Digestate at Different Pyrolysis Temperatures during OFMSW Anaerobic Digestion. Sustainability. **15**, 11917 (2023). https://doi.org/10.3390/su151511917
43. Waqas, W., Aburiazaiza, A.S., Miandad, R., Rehan, M., Barakat, M.A., Nizami, A.S.: Development of biochar as fuel and catalyst in energy recovery technologies. J. Clean. Prod. **188**, 477–488 (2018). https://doi.org/10.1016/j.jclepro.2018.04.017
44. Ibitoye, S.E., Loha, C., Mahamood, R.M., Jen, T.-C., Alam, M., Sarkar, I., et al.: An overview of biochar production techniques and application in iron and steel industries. Bioresour Bioproc. **11**, 65 (2024). https://doi.org/10.1186/s40643-024-00779-z
45. Afessa, M.M., Olu, F.E., Geleta, W.S., Legese, S.S., Venkata Ramayya, A.: Unlocking the potential of biochar derived from coffee husk and khat stem for catalytic tar cracking during biomass pyrolysis: characterization and evaluation. Biomass Conv Bioref. **15**, 11011–11026 (2025). https://doi.org/10.1007/s13399-024-05957-9
46. Chaturvedi, S., Singh, S.V., Dhyani, V.C., Govindaraju, K., Vinu, V., Mandal, S.: Characterization, bioenergy value, and thermal stability of biochars derived from diverse agriculture and forestry lignocellulosic wastes. Biomass Conv Bioref. **13**, 879–892 (2023). https://doi.org/10.1007/s13399-020-01239-2
47. Teng, W., Yu, Z., Shen, G., Ni, H., Zhang, X., Ma, X.: Microwave-assisted co-pyrolysis of eucalyptus wood and polypropylene for hydrocarbon-rich bio-oil based on multilayer MFI nanosheets catalysis. Energy. **317**, 134635 (2025). https://doi.org/10.1016/j.energy.2025.134635
48. Muddasar, M., Culebras, M., Collins, M.N.: Lignin and its carbon derivatives: Synthesis techniques and their energy storage applications. Mat. Today Sustain. **28**, 100990 (2024). https://doi.org/10.1016/j.mtsust.2024.100990
49. Wijitkosum, S., Sriburi, T.: Aromaticity, polarity, and longevity of biochar derived from disposable bamboo chopsticks waste for environmental application. Heliyon 9, e19831 (2023). https://doi.org/10.1016/j.heliyon.2023.e19831
50. Zhang, X., Zhang, P., Yuan, X., Li, Y., Han, L.: Effect of pyrolysis temperature and correlation analysis on the yield and physicochemical properties of crop residue biochar. Bioresour Technol. **296**, 122318 (2020). https://doi.org/10.1016/j.biortech.2019.122318
51. Ain, Q.U., Shafiq, M., Capareda, S.C., Bareen, F.E.: Effect of different temperatures on the properties of pyrolysis products of *Parthenium hysterophorus*. J. Saudi Chem. Societ. **25**, 101197 (2021). https://doi.org/10.1016/j.jscs.2021.101197
52. Yargicoglu, E.N., Sadasivam, B.Y., Reddy, K.R., Spokas, K.: Physical and chemical characterization of waste wood derived biochars. Waste Manag. **36**, 256–268 (2015). https://doi.org/10.1016/j.wasman.2014.10.029
53. Yi, S., Gao, B., Sun, Y., Wu, J., Shi, X., Wu, B., Hu, X.: Removal of levofloxacin from aqueous solution using rice-husk and wood-chip biochars. Chemosphere. **150**, 694–6701 (2016). https://doi.org/10.1016/j.chemosphere.2015.12.112
54. Sun, J., Tu, S., Lu, X., Li, X.: Coupling of Biochar and Manure Improves Soil Carbon Pool Stability, Pore Structure, and Microbial Diversity. Agronomy. **15**, 1384 (2025). https://doi.org/10.3390/agronomy15061384
55. Sang, Y., Chen, H., Khalifeh, M., Li, Y.: Catalysis and chemistry of lignin depolymerization in alcohol solvents - A review. Catal. Today. **408**, 168–181 (2023). https://doi.org/10.1016/j.cattod.2022.06.005
56. Chen, X., Wu, W., Han, L., Gu, M., Li, J., Chen, M.: Carbon stability and mobility of ball milled lignin- and cellulose-rich biochar colloids. Sci. Total Environ. **808**, 149759 (2022). https://doi.org/10.1016/j.scitotenv.2021.149759
57. Jalali, M., Panam, Z., Jalali, M., Buss, W.: The impact of feedstock type and pyrolysis parameters on the physical and chemical properties of biochars for sorption, agricultural and carbon sequestration applications: A meta-analysis. J. Anal. Appl. Pyrol. **192**, 107271 (2025). https://doi.org/10.1016/j.jaap.2025.107271
58. Leng, L., Huang, H.: An Overview of the Effect of Pyrolysis Process Parameters on Biochar Stability. Bioresour Technol. **270**, 627–642 (2018). https://doi.org/10.1016/j.biortech.2018.09.030
59. Nakason, K., Pathomrotsakun, J., Kraithong, W., Khemthong, P., Panyapinyopol, B.: Torrefaction of agricultural wastes: influence of lignocellulosic types and treatment temperature on fuel properties of biochar. Int. Energy J. **19**, 253–266 (2019)
60. Sharma, T., Hakeem, I.G., Gupta, A.B., Joshi, J., Shah, K., Vuppaladadiyam, A.K., Sharma, A.: Parametric influence of process conditions on thermochemical techniques for biochar production: A state-of-the-art review. J. Energy Inst. **113**, 101559 (2024). https://doi.org/10.1016/j.joei.2024.101559
61. Sun, X., Shan, R., Li, X., Pan, J., Liu, X., Deng, R., Song, J.: Characterization of 60 types of Chinese biomass waste and resultant biochars in terms of their candidacy for soil application. GCB Bioenergy. **9**, 1423–1435 (2017). https://doi.org/10.1111/gcbb.12435
62. Chen, D., Yu, X., Song, C., Pang, X., Huang, J., Li, Y.: Effect of pyrolysis temperature on the chemical oxidation stability of bamboo biochar. Bioresour Technol. **218**, 1303–1306 (2016). https://doi.org/10.1016/j.biortech.2016.07.112

63. Shi, Y., Zhu, Y., You, Z., Li, W., Wang, Y., Song, Y.: Evolution mechanism of organic macromolecular structure during lignite pyrolysis. J. Anal. Appl. Pyrol. **181**, 106643 (2024). https://doi.org/10.1016/j.jaap.2024.106643
64. Kim, K.H., Kim, J.Y., Cho, T.S., Choi, J.W.: Influence of pyrolysis temperature on physicochemical properties of biochar obtained from the fast pyrolysis of pitch pine (*Pinus rigida*). Bioresour Technol. **181**, 158–162 (2012). https://doi.org/10.1016/j.biortech.2012.04.094
65. Liu, Y., Zhao, X., Li, J., Ma, D., Han, R.: Characterization of biochar from pyrolysis of wheat straw and its evaluation on methylene blue adsorption. Desal Water Treat. **46**, 115–123 (2012). https://doi.org/10.1080/19443994.2012.677408
66. Chojnacka, A., Szczęsny, P., Błaszczyk, M.K., Zielenkiewicz, U., Detman, A., Salamon, A., et al.: Noteworthy Facts about a Methane-Producing Microbial Community Processing Acidic Effluent from Sugar Beet Molasses Fermentation. PLoS ONE. **10**, e0128008 (2015). https://doi.org/10.1371/journal.pone.0128008
67. Logan, M., Ravishankar, H., Tan, L.C., Lawrence, J., Fitzgerald, D., Lens, P.N.L.: Anaerobic digestion of dissolved air floatation slurries: Effect of substrate concentration and pH. Environ. Technol. Inn. **21**, 101352 (2021). https://doi.org/10.1016/j.eti.2020.101352
68. Poerschmann, J., Weiner, B., Koehler, R., Kopinke, F.D.: Organic breakdown products resulting from hydrothermal carbonization of brewer's spent grain. Chemosphere. **131**, 71–77 (2015). https://doi.org/10.1016/j.chemosphere.2015.02.057
69. Gao, S., Huang, Y., Yang, L., Wang, H., Zhao, M., Xu, Z., et al.: Evaluation the anaerobic digestion performance of solid residual kitchen waste by $NaHCO_3$ buffering. Energy Conv Manag. **93**, 166–174 (2015). https://doi.org/10.1016/j.enconman.2015.01.010
70. Jiang, M., Qiao, W., Wang, Y., Zou, T., Lin, M., Dong, R.: Balancing acidogenesis and methanogenesis metabolism in thermophilic anaerobic digestion of food waste under a high loading rate. Sci. Total Environ. **824**, 153867 (2022). https://doi.org/10.1016/j.scitotenv.2022.153867
71. Yellezuome, D., Zhu, X., Liu, X., Liu, R., Sun, C., Abd-Alla, M.H., et al.: Acidogenic gas utilization improves methane production in high-load digestion: Underlying mechanisms. Ren. Sustain. Energy Rev. 114698 (2024). (2021). https://doi.org/10.1016/j.rser.2024.114698
72. Wu, X., Zhou, Y., Liang, M., Lu, X., Chen, G., Zan, F.: Insights into the role of biochar on the acidogenic process and microbial pathways in a granular sulfate-reducing up-flow sludge bed reactor. Bioresour Technol. **355**, 127254 (2022). https://doi.org/10.1016/j.biortech.2022.127254
73. Sun, X., Atiyeh, H.K., Kumar, A., Zhang, H.R., Tanner, S.: Biochar enhanced ethanol and butanol production by *Clostridium carboxidivorans* from syngas. Bioresour Technol. **265**, 128–138 (2018). https://doi.org/10.1016/j.biortech.2018.05.106
74. Ding, J., Zhen, F., Kong, X., Hu, Y., Zhang, Y., Gong, L.: Effect of Biochar in Modulating Anaerobic Digestion Performance and Microbial Structure Community of Different Inoculum Sources. Fermentation. **10**, 151 (2024). https://doi.org/10.3390/fermentation10030151
75. Meng, L., Xie, L., Suenaga, T., Riya, S., Terada, A., Hosomi, M.: Eco-compatible biochar mitigates volatile fatty acids stress in high load thermophilic solid-state anaerobic reactors treating agricultural waste. Bioresour Technol. **309**, 123366 (2020). https://doi.org/10.1016/j.biortech.2020.123366
76. Ye, Z., Zhang, H., Lin, X., Huang, S., Zou, S., Zou, X.: Effect of Biochar Using N, P, and K Fertilisers on Growth and Quality of *Lithocarpus litseifolius*. Agronomy. **14**, 728 (2024). https://doi.org/10.3390/agronomy14040728
77. Zhong, H., Jiang, C., He, X., He, J., Zhao, Y., Chen, Y., et al.: Simultaneous change of microworld and biofilm formation in constructed wetlands filled with biochar. J. Environ. Manag. **349**, 119583 (2024). https://doi.org/10.1016/j.jenvman.2023.119583
78. Zhang, B., Zhang, J., Wang, Y., Qu, J., Jiang, Z., Zhang, X., et al.: Biodegradation of atrazine with biochar-mediated functional bacterial biofilm: Construction, characterization and mechanisms. J. Hazard. Mat. **465**, 133237 (2024). https://doi.org/10.1016/j.jhazmat.2023.133237
79. Wang, W.T., Dai, L.C., Wu, B., Qi, B.F., Huang, T.F., Hu, G.Q., et al.: Biochar-mediated enhanced ethanol fermentation (BMEEF) in *Zymomonas mobilis* under furfural and acetic acid stress. Biotechnol. Biofuels. **13**, 28 (2020). https://doi.org/10.1186/s13068-020-1666-6
80. Sekoai, P.T., Chunilall, V., Sithole, B., Habimana, O., Ndlovu, S., Ezeokoli, O.T., et al.: Elucidating the Role of Biofilm-Forming Microbial Communities in Fermentative Biohydrogen Process: An Overview. Microorganisms. **10**, 1924 (2022). https://doi.org/10.3390/microorganisms10101924
81. Tahsini, M.J., Nikaeen, M., Mohammadi, F., Taghipour, A., Tahmasebi, M., Nafez, A.H.: Composting of municipal solid waste with microbial-inoculated biochar amendment: impact on process and end-product quality. Biochar. **7**, 25 (2025). https://doi.org/10.1007/s42773-025-00426-6
82. Valentin, M.T., Białowiec, A.: Impact of using glucose as a sole carbon source to analyze the effect of biochar on the kinetics of biomethane production. Sci. Rep. **8656**, 14 (2024). https://doi.org/10.1038/s41598-024-59313-y
83. Caporaso, J.G., Lauber, C.L., Walters, W.A., Berg-Lyons, D., Huntley, J., Fierer, N.: Ultra-high-throughput microbial community analysis on the Illumina HiSeq and MiSeq platforms. ISME J. **6**, 1621–1624 (2012). https://doi.org/10.1038/ismej.2012.8
84. Callahan, B.J., McMurdie, P.J., Rosen, M.J., Han, A.W., Johnson, A.J.A., Holmes, S.P.: DADA2: high-resolution sample inference from Illumina amplicon data. Nat. Methods. **13**, 581–583 (2016). https://doi.org/10.1038/nmeth.3869
85. Cayuela, M.L., Van Zwieten, L., Singh, B.P., Jeffery, S., Roig, A., Sánchez-Monedero, M.A.: Biochar's role in mitigating soil nitrous oxide emissions: a review and meta-analysis. Agri Eco Environ. **191**, 5–16 (2014). https://doi.org/10.1016/j.agee.2013.10.009
86. Quast, C., Pruesse, E., Yilmaz, P., Gerken, J., Schweer, T., Yarza, P., Peplies, J., et al.: The SILVA ribosomal RNA gene database project: improved data processing and web-based tools. Nucleic Acids Res. **41**, D590–D596 (2013). https://doi.org/10.1093/nar/gks1219
87. Edgar, R.C.: UPARSE: highly accurate OTU sequences from microbial amplicon reads. Nat. Methods. **10**, 996–998 (2013). https://doi.org/10.1038/nmeth.2604
88. Fierer, N., Bradford, M.A., Jackson, R.B.: Toward an ecological classification of soil bacteria. Ecology. **88**, 1354–1364 (2007)
89. Janssen, P.H.: Identifying the dominant soil bacterial taxa in libraries of 16S rRNA and 16S rRNA genes. Appl. Environ. Microbiol. **72**, 1719–1728 (2006). https://doi.org/10.1128/AEM.72.3.1719-1728.2006
90. Vandamme, P., Dewhirst, F.E., Paster, B.J., On, S.L.: Genus I. *Arcobacter*. In: D.R. Boone, R.W. Castenholz (Eds.) Bergey's Manual of Systematic Bacteriology, pp. 1161–1165. Springer, New York (2005) (2005)
91. Delmont, T.O., Quince, C., Shaiber, A., Esen, Ö.C., Lee, S.T.M., Rappé, M.S., et al.: Nitrogen-fixing populations of Planctomycetes and Proteobacteria are abundant in surface ocean metagenomes. Nat. Microbiol. **3**, 804–813 (2018). https://doi.org/10.1038/s41564-018-0176-9
92. Rodríguez, H., Fraga, R.: Phosphate solubilizing bacteria and their role in plant growth promotion. Biotechnol. Adv. **17**, 319–339 (1999). https://doi.org/10.1016/S0734-9750(99)00014-2
93. Sharma, S.B., Sayyed, R.Z., Trivedi, M.H., Gobi, T.A.: Phosphate solubilizing microbes: sustainable approach for managing

phosphorus deficiency in agricultural soils. SpringerPlus. **2**, 587 (2013). https://doi.org/10.1186/2193-1801-2-587
94. Gaogane, G.J., Sekoai, P., Trois, C.: Sustainable Hydrogen Production via Dark Fermentation of Protein- and Lipid-Rich Municipal Organic Waste: Digestate Reuse and Ammonia Mitigation Strategies. Fermentation. **11**, 623 (2025). https://doi.org/10.3390/fermentation11110623
95. Yu, Y., Feng, S., Zhou, C., Yang, Y., Zhang, T.: Integrating hydrothermal pretreatment and co-digestion of activated sludge and kitchen waste for enhanced biogas production and microbial mechanism explanation. J. Environ. Manag. **389**, 126136 (2025). https://doi.org/10.1016/j.jenvman.2025.126136
96. Liu, H., Liang, H., Liu, Y., Zhang, H., Han, H., Xin, B., et al.: *Alicycliphilus* soli sp. nov., Isolated from a Plastic Film Greenhouse Soil and the Proposal for the Reclassification of *Diaphorobacter limosus* as *Alicycliphilus limosus* comb. nov. Curr. Microbiol. **82**, 443 (2025). https://doi.org/10.1007/s00284-025-04430-8
97. Wexler, H.M.: Bacteroides: the good, the bad, and the nitty-gritty. Clin. Microbiol. Rev. **20**, 593–621 (207). https://doi.org/10.1128/cmr.00008-07
98. Pérez-Cataluña, A., Salas-Massó, N., Diéguez, A.L., Balboa, S., Lema, A., Romalde, J.S., et al.: Revisiting the taxonomy of the genus *Arcobacter*: getting order from the chaos. Front. Microbiol. **9**, 2077 (2018). https://doi.org/10.3389/fmicb.2018.02077
99. Gerritsen, J., Hornung, B., Renckens, B., van Hijumet, S.A.F.T., dos Santos, V.A.P.M., Rijkers, G.T., et al.: Genomic and functional analysis of *Romboutsia ilealis* CRIB T reveals adaptation to the small intestine. PeerJ. **5**, e3698 (2017). https://doi.org/10.7717/peerj.3698
100. Kang, S.M., Radhakrishnan, R., You, Y., et al.: Phosphate solubilizing Bacillus megaterium mj1212 regulates endogenous plant carbohydrates and amino acids contents to promote mustard plant growth. Indian J. Microbiol. **54**, 427–433 (2014). https://doi.org/10.1007/s12088-014-0476-6
101. Ferreira, S., Queiroz, J.A., Oleastro, M., Domingues, F.C.: Insights in the pathogenesis and resistance of Arcobacter: a review. Crit. Rev. Microbiol. **42**, 364–383 (2016). https://doi.org/10.3109/1040841X.2014.954523
102. Kolton, M., Harel, Y.M., Pasternak, Z., Graber, E.R., Elad, Y., Cytryn, E.: Impact of biochar application to soil on the root-associated bacterial community structure of fully developed greenhouse pepper plants. Appl. Environ. Microbiol. **77**, 4924–4930 (2011). https://doi.org/10.1128/AEM.00148-11
103. Gerritsen, J., Fuentes, S., Grievink, W., van Niftrik, L., Tindall, B.J., Timmerman, H.M., et al.: Characterization of Romboutsia ilealis gen. nov., sp. nov., isolated from the gastro-intestinal tract of a rat, and proposal for the reclassification of five closely related members of the genus Clostridium into the genera Romboutsia gen. nov., Intestinibacter gen. nov., Terrisporobacter gen. nov. and Asaccharospora gen. nov. Int. J. Syst. Evol. Microbiol. **64**, 1600–1616 (2014). https://doi.org/10.1099/ijs.0.059543-0
104. Lozupone, C., Knight, R.: UniFrac: a new phylogenetic method for comparing microbial communities. Appl. Environ. Microbiol. **71**, 8228–8235 (2005). https://doi.org/10.1128/AEM.71.12.8228-8235.2005
105. Kayoumu, M., Wang, H., Duan, G.: Interactions between microbial extracellular polymeric substances and biochar, and their potential applications: a review. Biochar. **7**, 62 (2025). https://doi.org/10.1007/s42773-025-00452-4
106. Chen, J., Li, S., Liang, C., Xu, Q., Li, Y., Qin, H., et al.: Response of microbial community structure and function to short-term biochar amendment in an intensively managed bamboo (*Phyllostachys praecox*) plantation soil: effect of particle size and addition rate. Sci. Total Environ. **574**, 24–33 (2017). https://doi.org/10.1016/j.scitotenv.2016.08.190
107. Ding, Y., Liu, Y., Liu, S., Li, Z., Tan, X., Huang, X.: Biochar to improve soil fertility, A review. Agron. Sustain. Develop. **36**, 36 (2016). https://doi.org/10.1007/s13593-016-0372-z
108. McInerney, M.J., Struchtemeyer, C.G., Sieber, J., et al.: Physiology, ecology, phylogeny, and genomics of microorganisms capable of syntrophic metabolism. Annals New. York Acad. Sci. **1125**, 58–72 (2008). https://doi.org/10.1196/annals.1419.005
109. Meng, L., Cheng, Z., Wang, Y., Li, S., Clarke, N.: Arbuscular Mycorrhizal Fungal Interacted with Biochar and Enhanced Phosphate-Solubilizing Microorganism Abundance and Phosphorus Uptake in Maize. Agronomy. **14**, 1678 (2024). https://doi.org/10.3390/agronomy14081678
110. Gul, S., Whalen, J.K., Thomas, B.W., Sachdeva, V., Deng, H.: Physico-chemical properties and microbial responses in biochar-amended soils: mechanisms and future directions. Agr Ecosyst. Environ. **206**, 46–59 (2015). https://doi.org/10.1016/j.agee.2015.03.015
111. Western Cape Government: Business model: biomass products from alien invasive plants. Department of Environmental Affairs and Development Planning, Western Cape Government (2021)
112. Tongke Activated Carbon: How much does activated carbon cost?: (2025). https://www.tongkeac.com/how-much-does-activated-carbon-cost.html. Accessed 10 March 2026
113. Sekoai, P.T., Habimana, O.: Can biochar rescue Africa's soils and its crops? Nat. Afr. Comment. (2025). https://doi.org/10.1038/d44148-025-00295-y